TECHNICAL NOTE R-39

DETERMINATION OF TRAJECTORY PARAMETERS RELATIVE TO VARIOUS AROD GROUND STATIONS

Prepared By

H. M. Minshew
A. R. Phillips
H. C. Crews, Jr.

June, 1963

BROWN ENGINEERING COMPANY INC.
HUNTSVILLE, ALABAMA

TECHNICAL NOTE R-39

DETERMINATION OF TRAJECTORY PARAMETERS RELATIVE TO VARIOUS AROD GROUND STATIONS

June, 1963

Prepared For

INSTRUMENTATION BRANCH
ASTRIONICS DIVISION
GEORGE C. MARSHALL SPACE FLIGHT CENTER

By

SCIENTIFIC RESEARCH LABORATORIES
BROWN ENGINEERING COMPANY, INC.

Contract No. NAS8-2495

Prepared By

H. M. Minshew
A. R. Phillips
H. C. Crews, Jr.

ABSTRACT

The slant range, rate of change of slant range, the maximum slant range acceleration, $\ddot{R}$, elevation angle, maximum rate of change of elevation angle, azimuth angle, maximum rate of change of azimuth angle, aspect or look angle, and maximum rate of change of aspect angle as measured from six selected AROD ground stations are computed and given as a function of vehicle ground range and time from launch from Cape Canaveral for a 105 NM circular orbit trajectory on an initial bearing angle of 105 degrees.

For purposes of analyzing vehicle antenna pattern requirements, the missile azimuth and missile elevation angles are computed and presented for each station as a function of time and vehicle ground range from launch.

Approved:

Raymond C. Watson, Jr.
Director of Scientific Research

TABLE OF CONTENTS

LIST OF FIGURES

LIST OF FIGURES (Cont'd)

LIST OF FIGURES (Cont'd)

LIST OF FIGURES (Cont'd)

LIST OF SYMBOLS

E	East
$\bar{i}, \bar{j}, \bar{k}$	Unit vectors along the X, Y, Z axes respectively
N	North
$\bar{N}_1$	Vector normal to the plane containing $\bar{r}_1$ and $\bar{V}$
$\bar{N}_2$	Vector normal to the plane containing $\bar{R}$ and $\bar{V}$
O	Origin of the X, Y, Z axes
O_r	Origin of a coordinate system located at the radar site
$\bar{R}$	Position vector from O to the vehicle
$\ddot{R}$	Range-rate-rate (slant range acceleration)
$\bar{R}_e$	Radius of the earth in vector form
R_e	Magnitude of $\bar{R}_e$
$\bar{r}$	Position vector from O to the vehicle
r	Magnitude of $\bar{r}$
$\bar{r}_1$	Position vector from O_r to the vehicle
r_1	Magnitude of $\bar{r}_1$
$\dot{\bar{r}}_1$	Time rate of change of $\bar{r}_1$
rr_1	Range-rate (component of the velocity vector in the direction of r_1)
$\bar{V}$	Velocity vector in X, Y, Z system
V	Magnitude of $\bar{V}$
V_x, V_y, V_z	Components of $\bar{V}$ in the vehicle coordinate system

X, Y, Z	Earth centered coordinate system
$\dot{X}, \dot{Y}, \dot{Z}$	First time derivatives of X, Y, Z
X_r, Y_r, Z_r	Radar coordinate system
x, y, z	Vehicle local coordinate system

Greek Symbols

β	Vehicle bearing angle measured positive clockwise from earth
γ	Vehicle elevation angle (see page 10)
δ	Vehicle path angle measured from local vertical
η	Angle between the radar line-of-sight and the velocity vector
θ	Longitude of the vehicle
θ_N	Angle between the plane containing $\overline{r}_1$ and $\overline{V}$ and a second plane containing $\overline{R}$ and $\overline{V}$ (see page 11)
$\Delta\theta_N$	Angle representing the roll of the vehicle about its longitudinal axis
θ_S	Longitude of the station
μ	Vehicle azimuth angle (see page 10)
ξ	Elevation angle (see page 7)
ϕ	Latitude of the vehicle
ϕ_s	Latitude of the station
ψ	Azimuth angle (see page 8)
Ω	Earth's rotation rate

INTRODUCTION

Six ground stations were previously selected as potential AROD* transponder locations based on minimum geometric dilution of precision and continuous coverage for the launch phase of a 105 NM circular orbit trajectory launched from Cape Canaveral on an initial bearing angle of 105° from true north. (1)

In order to provide input data for design of the first space launched prototype of the AROD system, the ranges of values to be experienced on such a trajectory for slant range, range rate, maximum doppler rate (range acceleration), elevation angle, maximum elevation angular rate, azimuth angle, maximum azimuth angular rate, aspect angle and maximum rate of change of aspect angle with respect to each ground station were required. In addition, the elevation angle with respect to missile coordinates (the angle between the missile long axis and the projection of the position vector from each station in the vertical plane containing the axis) and the missile azimuth angle (the angle between the vertical plane through the missile axis and the position vector from each station) were required to analyze antenna pattern limitations. Methods for calculation of these parameters are derived and specific results are plotted for each of the six stations considered.

Reports to follow will give the details of the computer programs used. The basic program now has the capability of accepting any

*Airborne Range and Orbital Determination definitive trajectory data, choosing those ground stations visible above a pre-determined minimum elevation angle or horizon, calculating all the above trajectory parameters and taking all visible stations three at a time in the calculation of GDOP spherical error volume.

ANALYSIS

Figure 1 and the accompanying equations give the coordinate scheme used in relating the vehicle position and velocity to the earth-fixed system of coordinates. The relation of the vehicle position to the ground station location is given by the equations and notations of Figure 2, while Figure 3 indicates the method used to solve for the elevation angle ξ. Figure 4 shows the notation used to calculate the azimuth angle ψ and the aspect angle η. Figure 5 gives the notation used for the vehicle azimuth and elevation angles.

It should be noted that a spherical earth is assumed and trajectory positions and velocities may be furnished for either a fixed or rotating earth without affecting the calculation method.

The position velocity information used in these calculations was given at twenty second intervals which made the determination of higher time derivatives of range rate, elevation angle, azimuth angle, aspect angle, missile elevation angles and missile azimuth angles difficult. To obtain these derivatives, the parameter plots were smoothed and the slope of the curves were graphically determined.

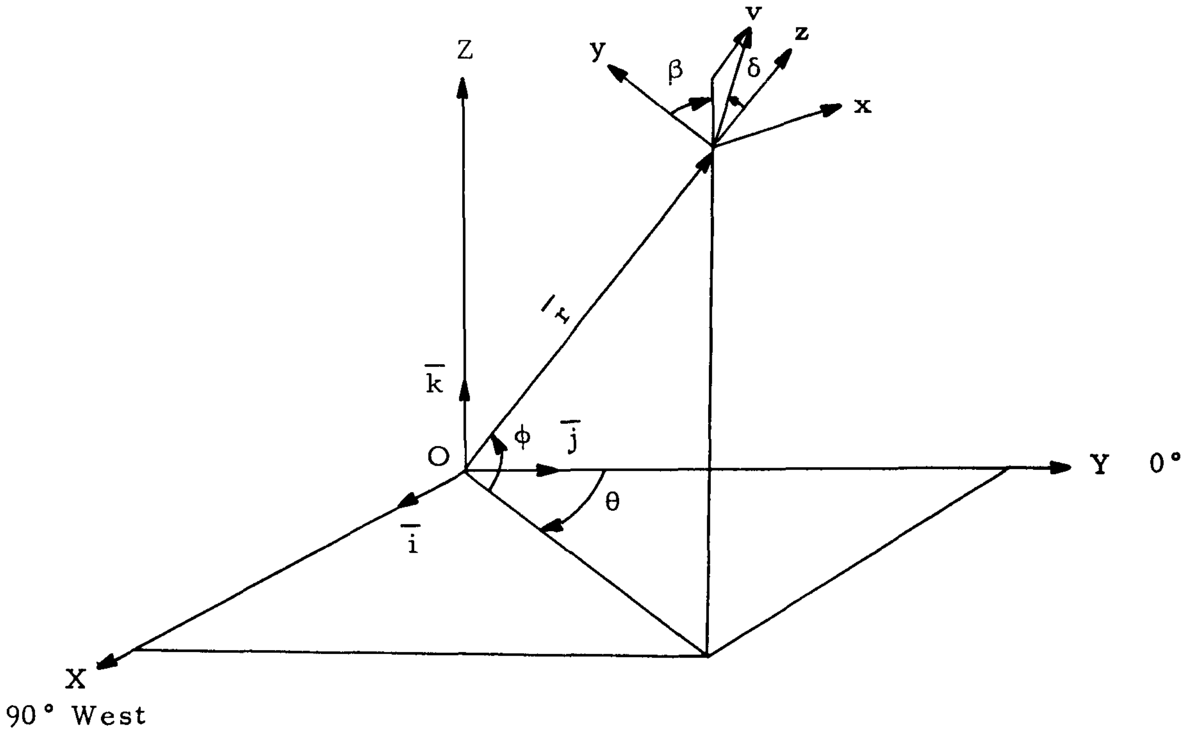

Figure 1

Vehicle Position and Velocity Relative to an Earth-fixed System

X, Y, Z — Earth-fixed co-ordinate system
X and Y are in the plane of the Equator
Z is along the polar axis

$\bar{i}$, $\bar{j}$, $\bar{k}$ — Unit vectors along X, Y, Z respectively

x, y, z — Local reference frame of vehicle
z is along $\bar{r}$.
x and y are perpendicular to $\bar{r}$; y is positive due North
$\bar{r} = X\bar{i} + Y\bar{j} + Z\bar{k}$
θ is the geocentric longitude of the vehicle
ϕ is the geocentric latitude of the vehicle
β is the bearing angle measured positive clockwise from North
δ is the path angle measured from the local vertical

Components of Velocity in the X, Y, Z System

(See Figure 1)

The components of V in the local reference frame of the vehicle (x, y, z) are given by:

$$V_x = V \sin \delta \sin \beta$$

$$V_y = V \sin \delta \cos \beta$$

$$V_z = V \cos \delta$$

$\dot{X}$, $\dot{Y}$, and $\dot{Z}$ in terms of V_x, V_y, and V_z are given by:

$$\dot{X} = - V_x \cos \theta - V_y \sin \phi \sin \theta + V_z \cos \phi \sin \theta$$

$$\dot{Y} = V_x \sin \theta - V_y \sin \phi \cos \theta + V_z \cos \phi \cos \theta$$

$$\dot{Z} = V_y \cos \phi + V_z \sin \phi$$

where ϕ and θ are the latitude and longitude of the vehicle.

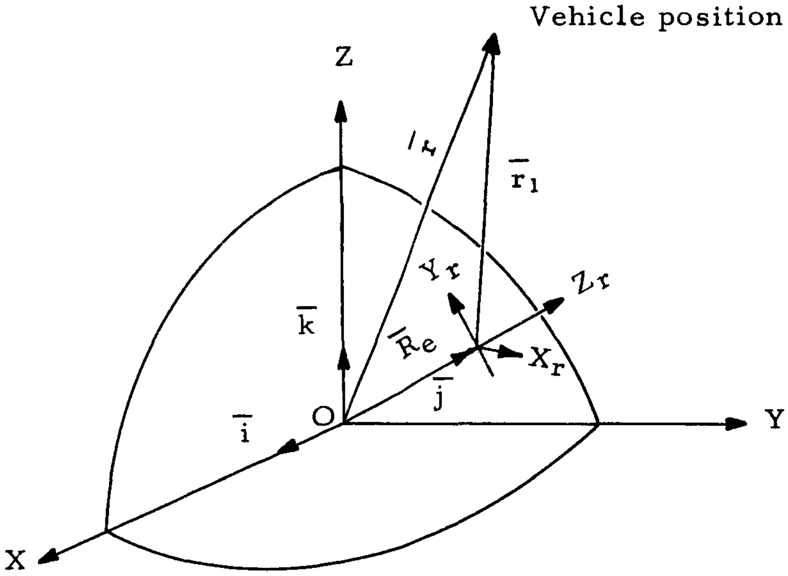

Figure 2

Range from a Point on the Earth's Surface to the Vehicle

X_r, Y_r, Z_r	Co-ordinate system fixed at the station
X_1, Y_1, Z_1	Co-ordinates of the station in the X, Y, Z system
$\bar{r}_1$	Range from the station to the vehicle
$\bar{R}_e$	Radius of the earth

X_1, Y_1, and Z_1 are given in terms of ϕ_s and θ_s by:

$$X_1 = R_e \cos\phi_s \sin\theta_s$$

$$Y_1 = R_e \cos\phi_s \cos\theta_s$$

$$Z_1 = R_e \sin\phi_s$$

$\bar{r}_1$ is determined by the following relation:

$$\bar{r}_1 = \bar{r} - \bar{R}_e$$

$$\bar{r}_1 = (X - X_1)\bar{i} + (Y - Y_1)\bar{j} + (Z - Z_1)\bar{k}$$

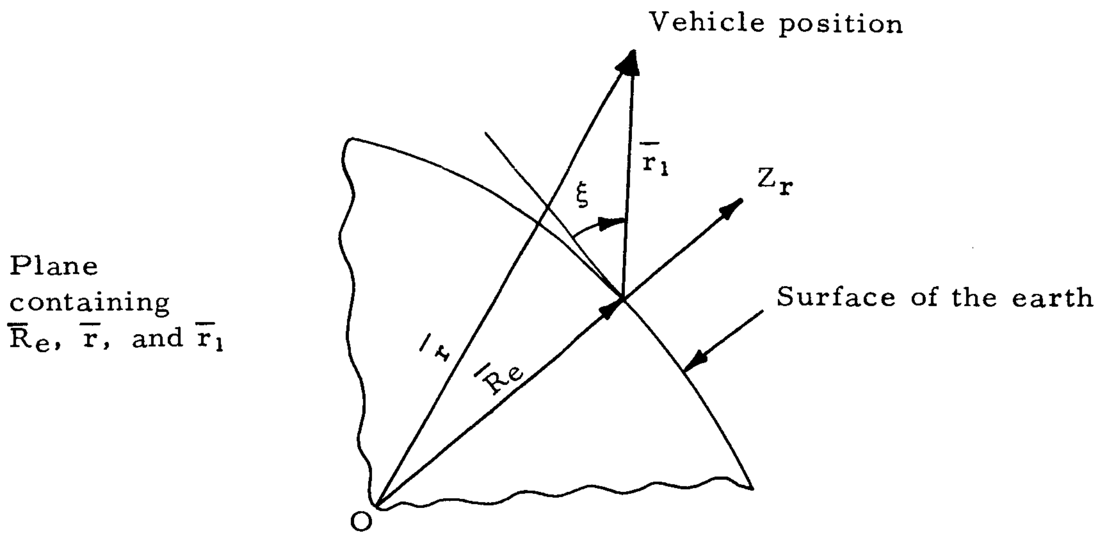

Figure 3

Elevation Angle (ξ)

The elevation angle is found by the law of cosines.

$$r^2 = R_e^2 + r_1^2 - 2 R_e r_1 \cos(\pi/2 + \xi)$$

or

$$r^2 = R_e^2 + r_1^2 + 2 R_e r_1 \sin \xi$$

$$\xi = \sin^{-1}\left[\frac{r^2 - R_e^2 - r_1^2}{2 R_e r_1}\right]$$

where r, r_1, and R_e are the magnitudes of the previously defined vectors, $\overline{r}$, $\overline{r}_1$, and $\overline{R}_e$.

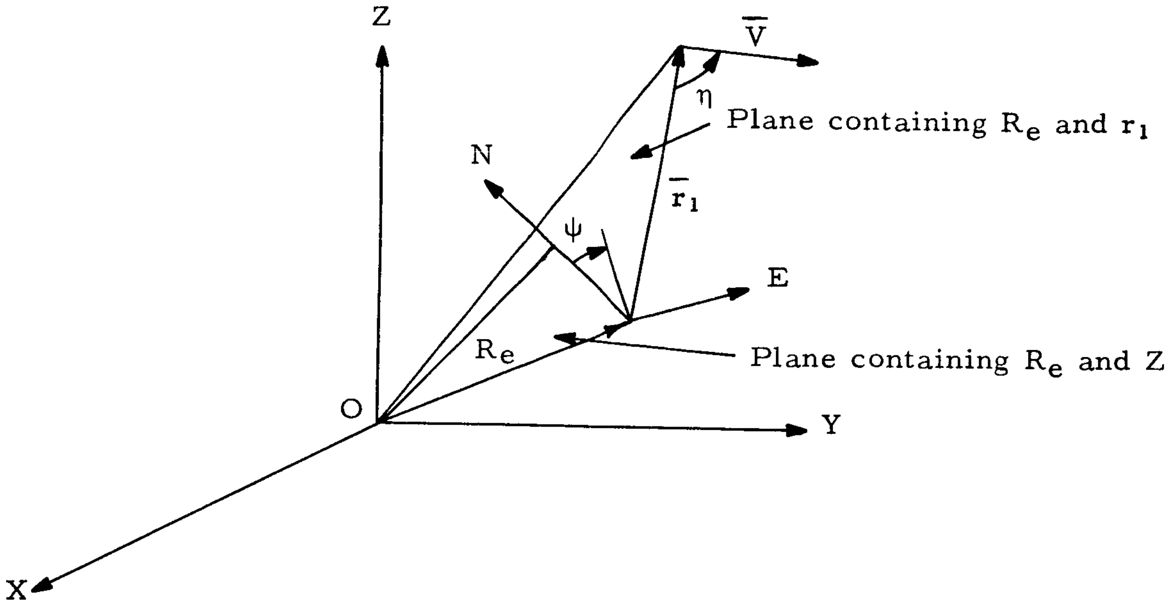

Figure 4

Azimuth Angle (ψ)

The azimuth angle, ψ, is computed from the following vector equations.

$\overline{k} \times \overline{R_e}$ gives a vector normal to the plane containing $\overline{k}$ and $\overline{R_e}$

$\overline{R_e} \times \overline{r_1}$ gives a vector normal to the plane containing $\overline{R_e}$ and $\overline{r_1}$

The angle between the planes is equal to the angle between the two normals and is given by the dot product of $(\overline{k} \times R_e)$ and $(\overline{R_e} \times \overline{r_1})$.

$$\psi = \cos^{-1}\left[\frac{(\overline{R_e} \times \overline{r}\ ) \cdot (\overline{k} \times \overline{R_e})}{|\overline{R_e} \times \overline{r_1}|\ |\overline{k} \times \overline{R_e}|}\right]$$

Aspect Angle (η) and Range Rate (rr_1)

$$\overline{V} = \dot{X}\overline{i} + \dot{Y}\overline{j} + \dot{Z}\overline{k}$$

The aspect angle is given by the dot product of $\overline{r}_1$ and $\overline{V}$.

$$\eta = \cos^{-1}\left[\frac{\overline{r}_1 \cdot \overline{V}}{|\overline{r}_1|\ |\overline{V}|}\right]$$

The range rate, rr_1, is the component of $\frac{d\overline{r}_1}{dt}$ along $\overline{r}_1$ and is given by:

$$rr_1 = \left|\dot{\overline{r}}_1\right| \cos\eta$$

where $\dot{\overline{r}}_1 = (\dot{X} + Y_1\Omega)\overline{i} + (\dot{Y} - X_1\Omega)\overline{j} + \dot{Z}\,\overline{i}$

The terms $Y_1\Omega$ and $X_1\Omega$ account for the fact that the stations are rotating with the earth at an angular speed of Ω radians per second.

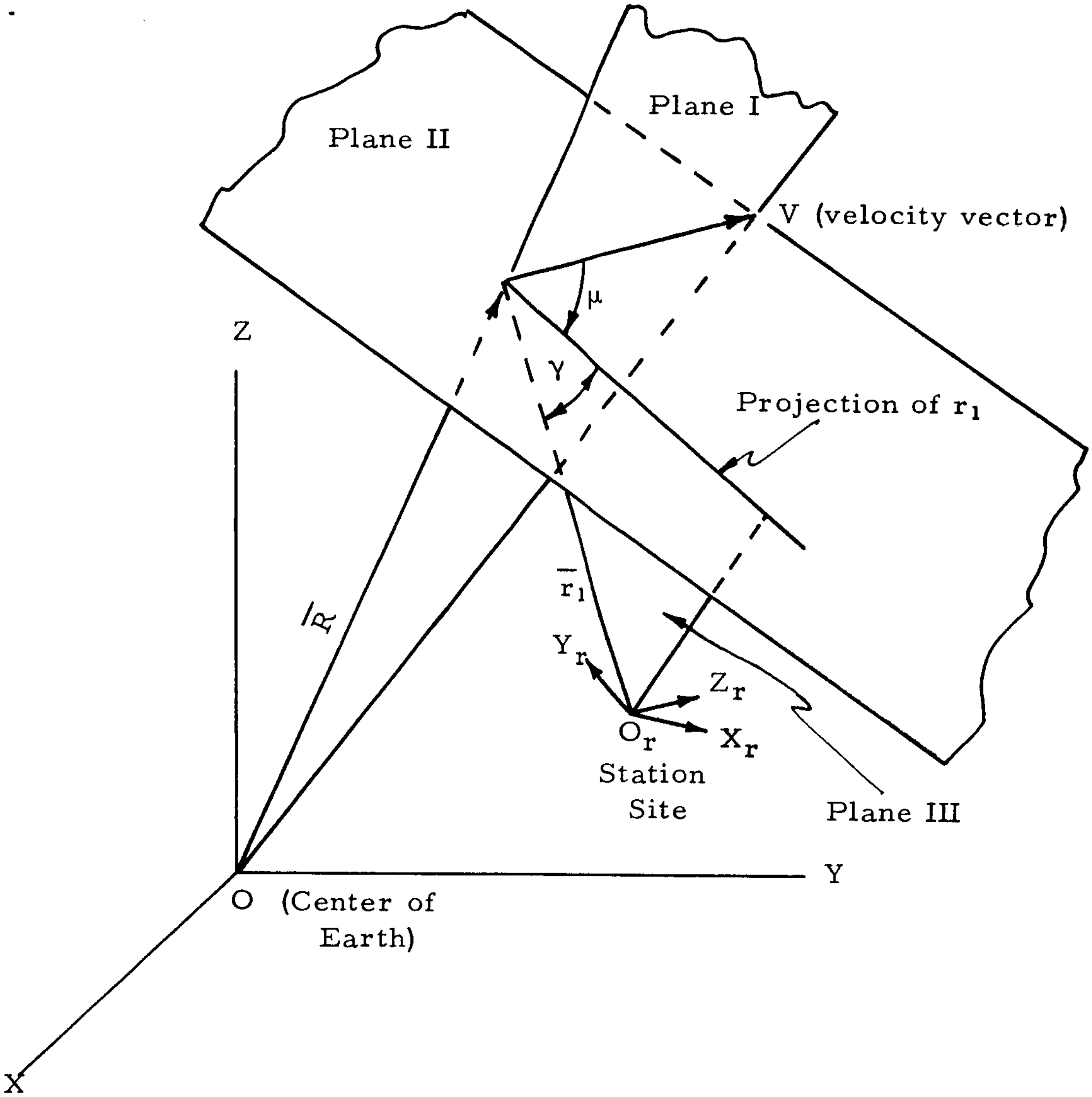

Figure 5 - Definition of Vehicle Azimuth Angle μ and Vehicle Elevation Angle γ

Plane I: A plane containing the radius vector $\overline{R}$, the vehicle velocity vector $\overline{V}$, and the origin O of an earth-centered co-ordinate system

Plane II: A plane which is perpendicular to Plane I and also contains the velocity vector

Plane III: A plane containing the radar range vector, $\overline{r_1}$, hence the origin of a co-ordinate system located at the station site, and perpendicular to Plane II.

γ = angle between Plane II and $\overline{r_1}$ in Plane III or the angle between $\overline{r_1}$ and its projection in Plane II

μ = angle between the projection of $\overline{r_1}$ in Plane II and the velocity vector

The vehicle azimuth angle (μ) is calculated from the following equation:

$$\mu = \tan^{-1} [\tan \eta \cos (\theta_N \bullet \Delta \theta_N)]$$

where

η is the aspect angle defined above

and

θ_N is the angle between a plane containing $\overline{r_1}$ and $\overline{V}$ and a second plane containing $\overline{R}$ and $\overline{V}$.

$\Delta \theta_N$ represents a roll of the vehicle about its longitudinal axis.

A normal to the plane containing $\overline{r_1}$ and $\overline{V}$ is given by

$$\overline{r_1} \times \overline{V} = \overline{N_1} \ ,$$

and a normal to the plane containing $\overline{R}$ and $\overline{V}$ is

$$\overline{R} \times \overline{V} = \overline{N_2} \ .$$

Since the angle between the normals is equal to the angle between the planes, θ_N is given by:

$$\theta_N = \cos^{-1} \frac{N_1 \cdot N_2}{|\overline{N_1}| \ |\overline{N_2}|}$$

The vehicle elevation angle (γ) is given by:

$$\gamma = \sin^{-1} [\sin \eta \sin (\theta_N \pm \Delta \theta_N)]$$

where

η, θ_N and $\Delta \theta_N$ are as defined above.

Figures 35 through 46 give γ and μ for vehicle roll angles of -5°, 0° and 5°.

PRESENTATION OF RESULTS

The slant range is given for each of the six stations as a function of time from launch in Figures 6 through 11. The rate of change of slant range is given for each station in Figures 12 through 17. The elevation angle for each station as a function of time from launch is given in Figures 18 through 23. Azimuth angles for each station are plotted in Figures 24 through 28 and aspect angles are given by Figures 29 through 34. Figures 35 through 40 give the vehicle azimuth angles for 0 and ± 5 degree roll. Figures 41 through 46 present the vehicle elevation angles as a function of time and roll limits. Ground range as a function of time from launch is given in Figure 47. Altitude as a function of time is given in Figure 48.

Table I presents the maximum values of the slopes of several of the parameters and the time or times of their occurrence.

Figure 6

Slant Range As Seen From Cape Canaveral
105 NM Orbit Launch Phase,
Initial Bearing 105 Degrees

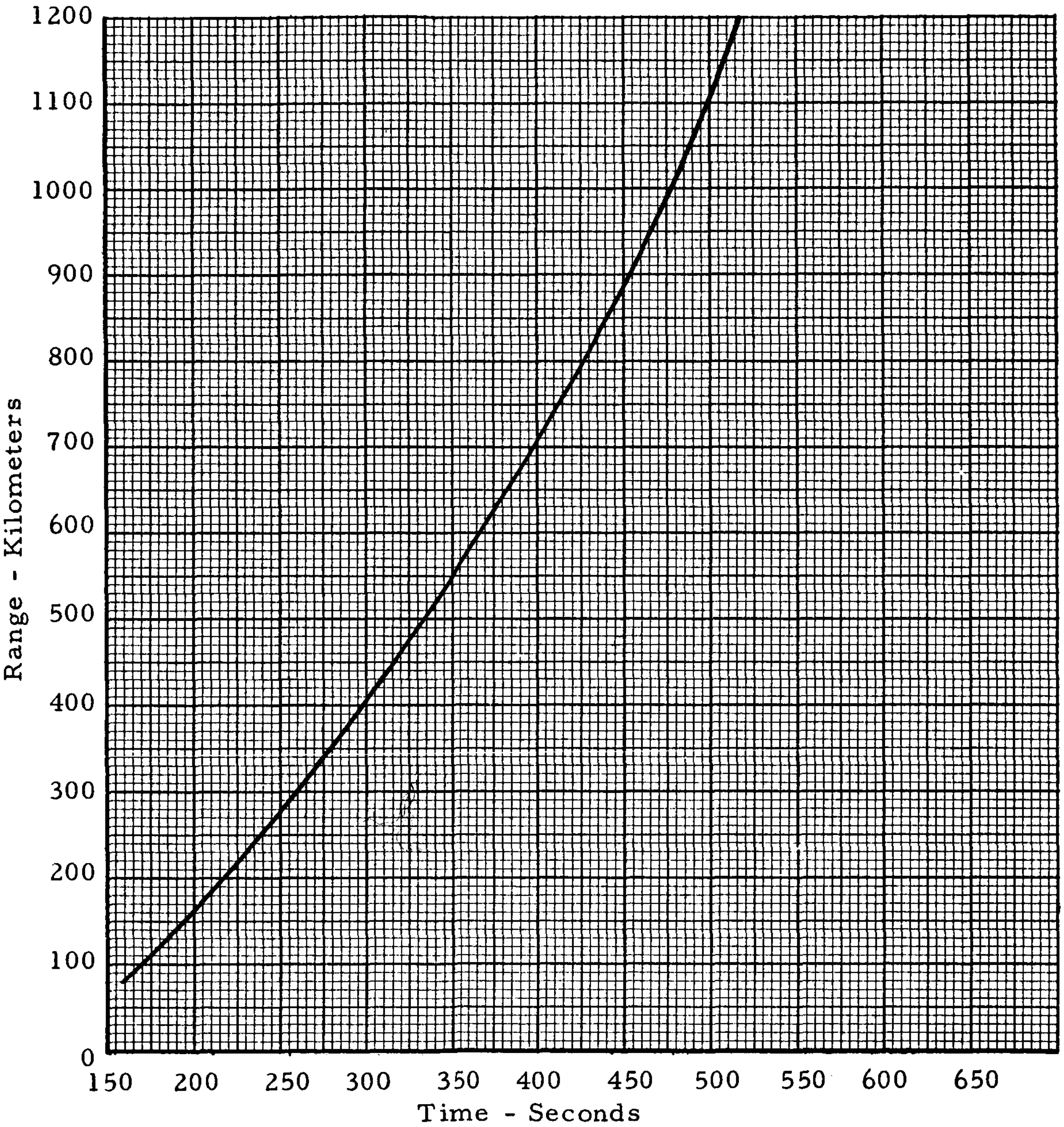

Figure 7

Slant Range As Seen From Site Jupiter
105 NM Orbit Launch Phase,
Initial Bearing 105 Degrees

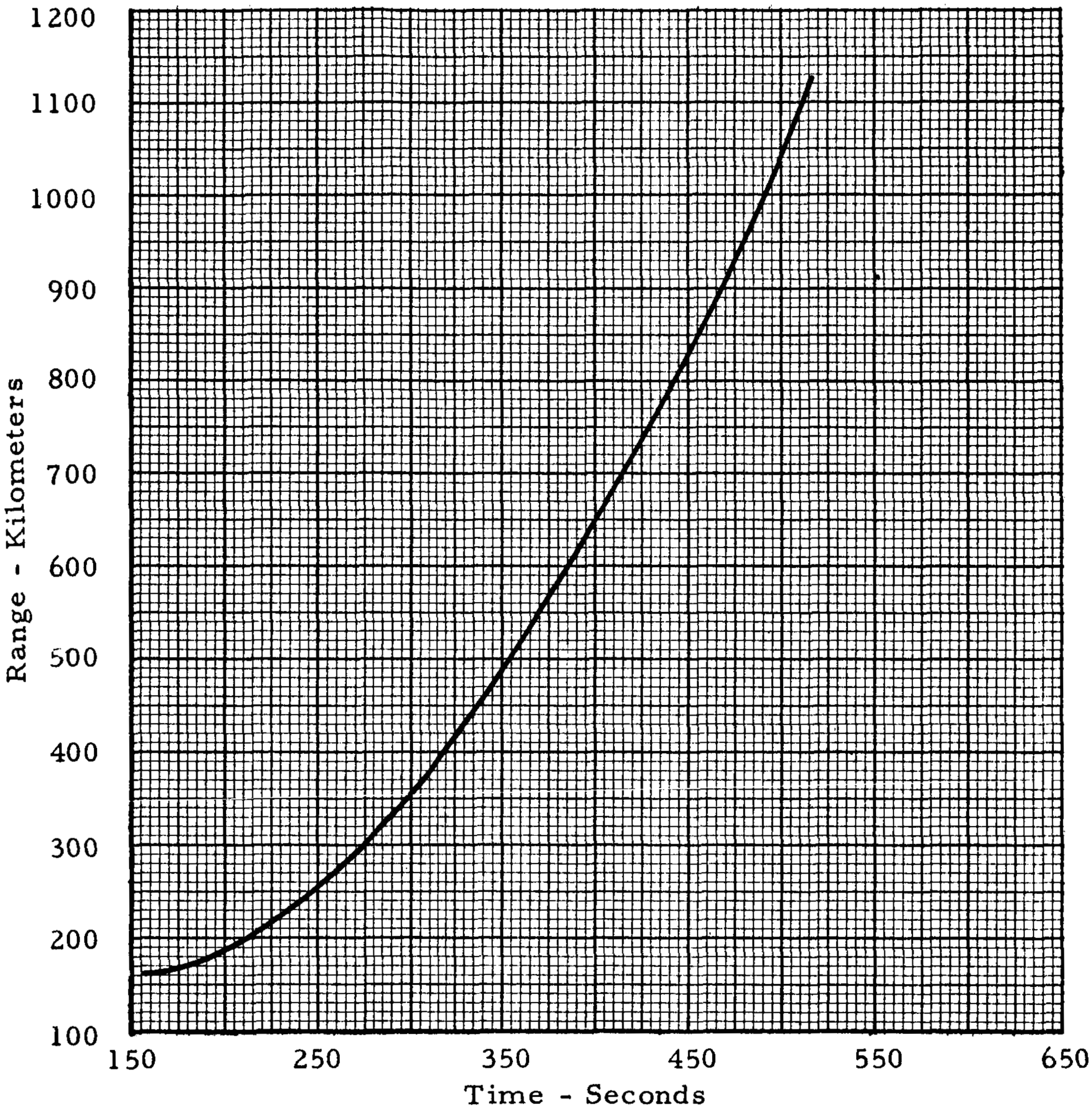

Figure 8

Slant Range As Seen From San Salvador
105 NM Orbit Launch Phase,
Initial Bearing 105 Degrees

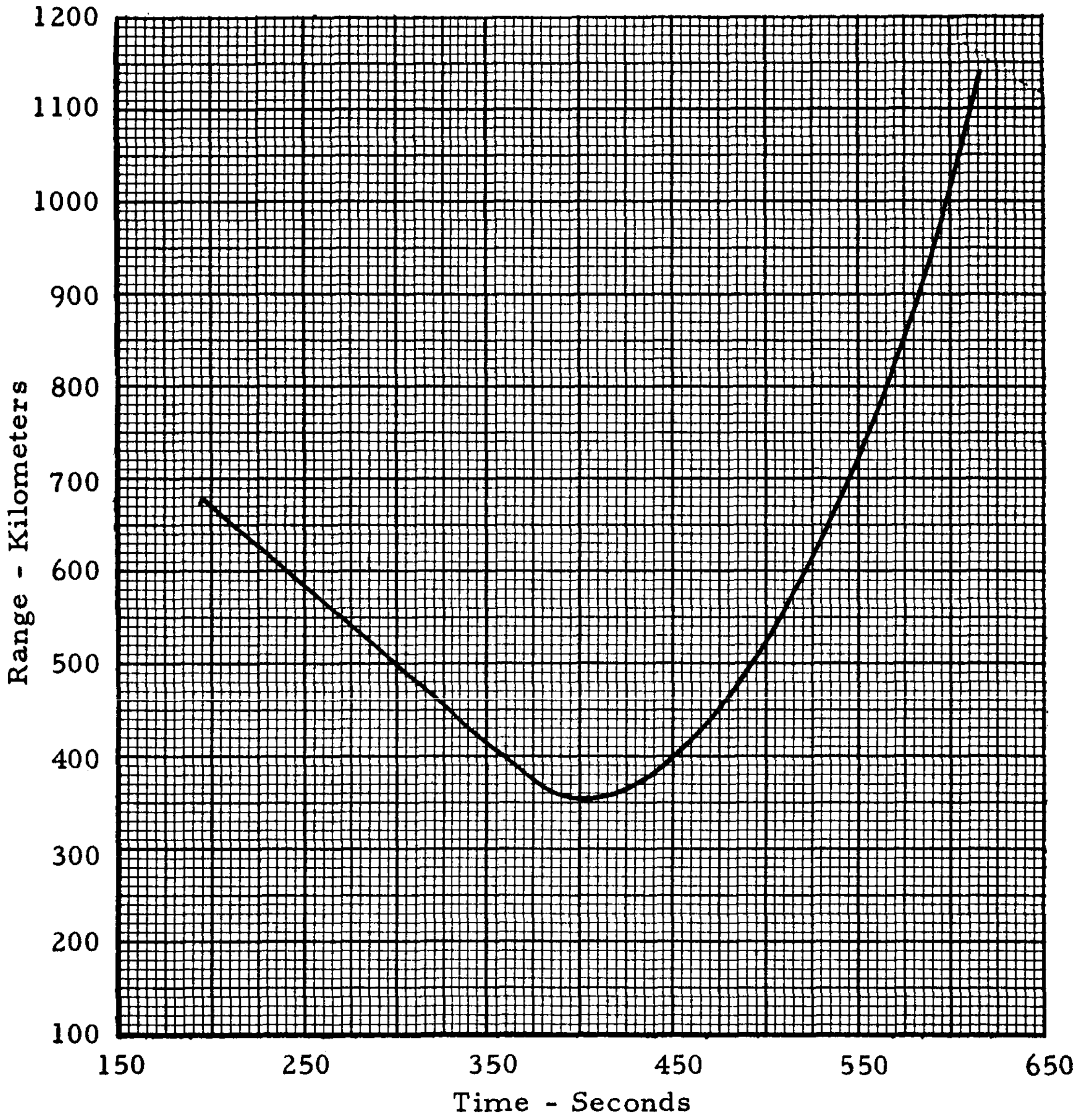

Figure 9

Slant Range As Seen From Grand Turk
105 NM Orbit Launch Phase,
Initial Bearing 105 Degrees

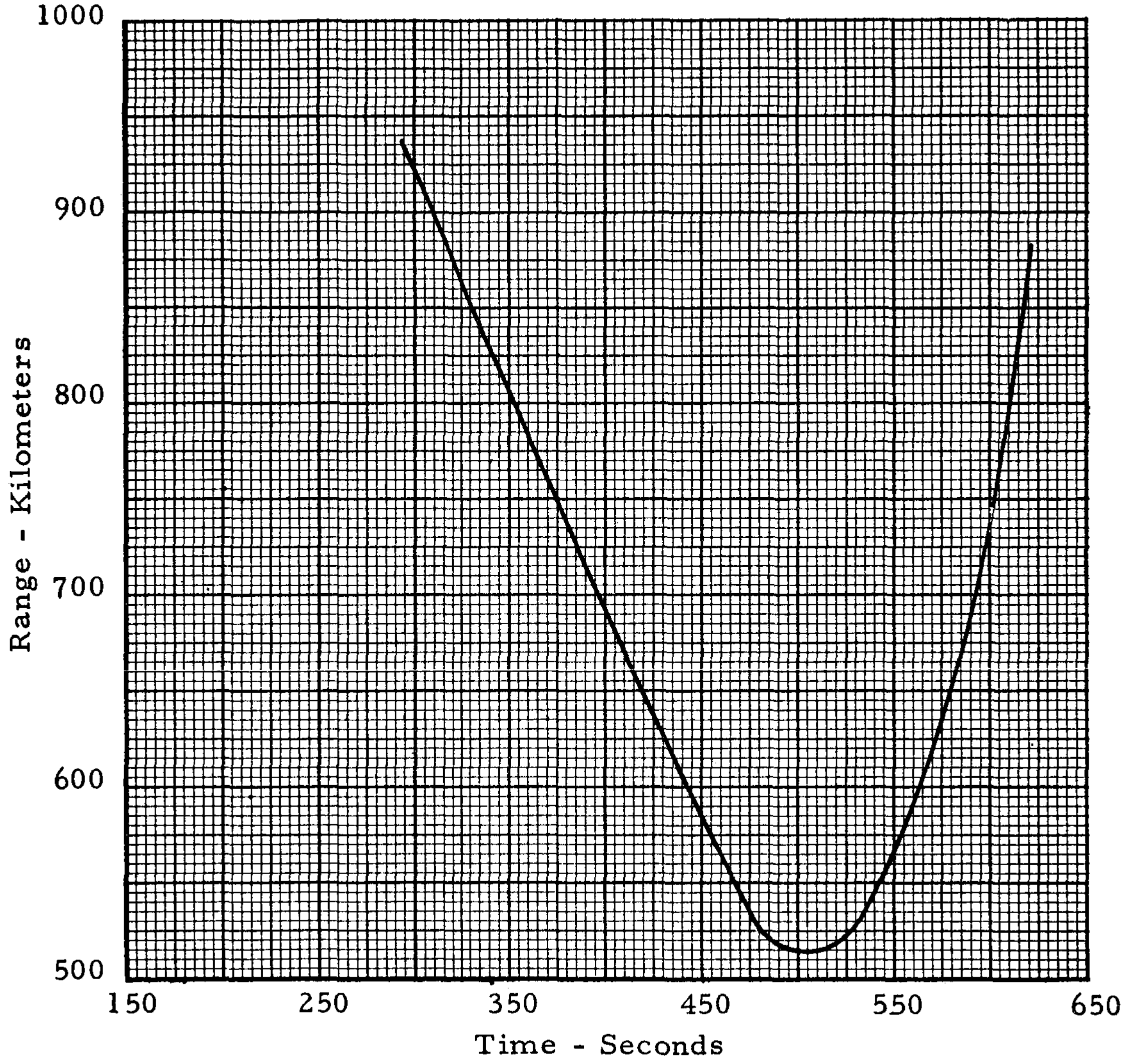

Figure 10

Slant Range As Seen From Bermuda
105 NM Orbit Launch Phase,
Initial Bearing 105 Degrees

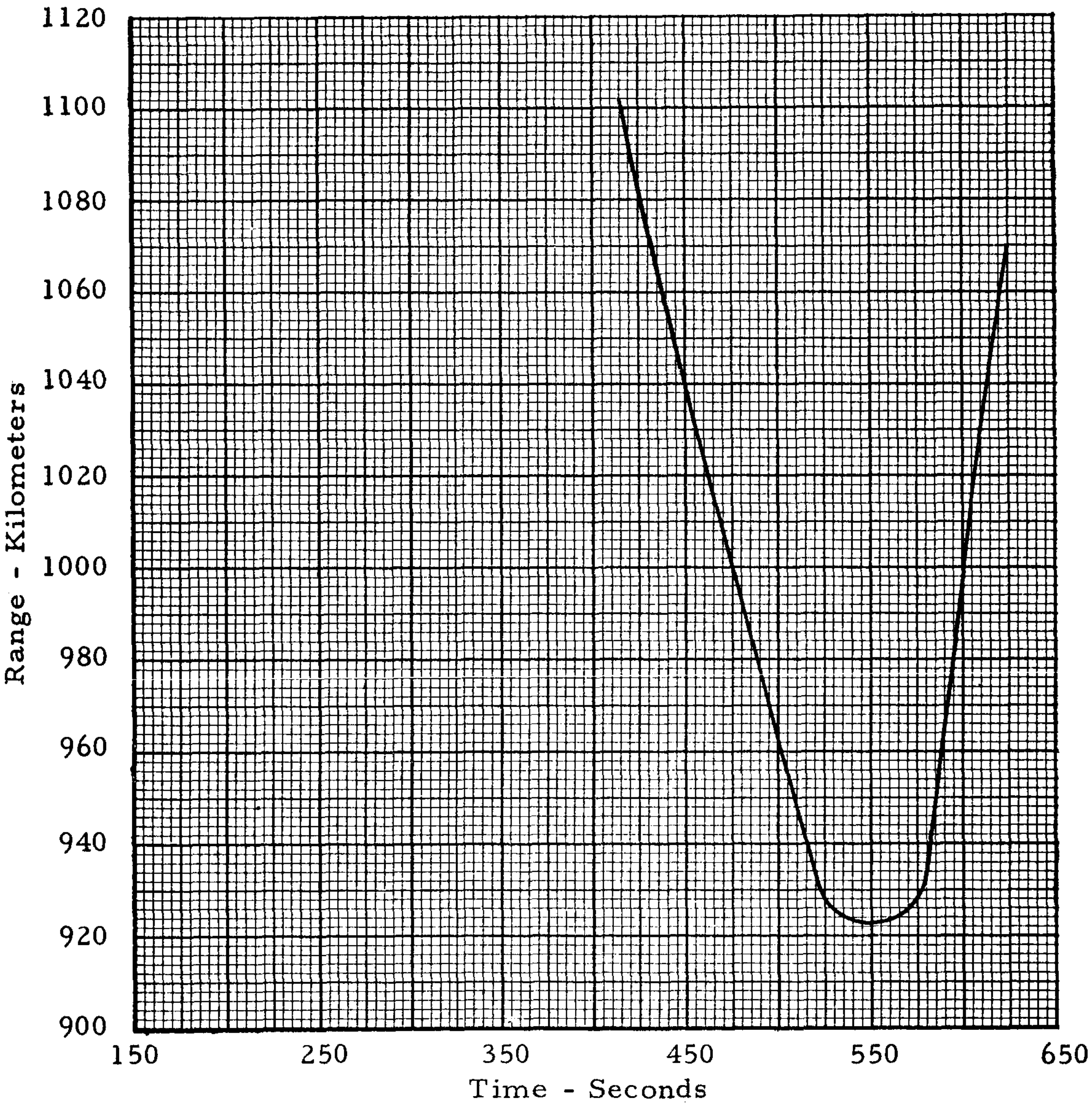

Figure 11

Slant Range As Seen From Antigua
105 NM Orbit Launch Phase,
Initial Bearing 105 Degrees

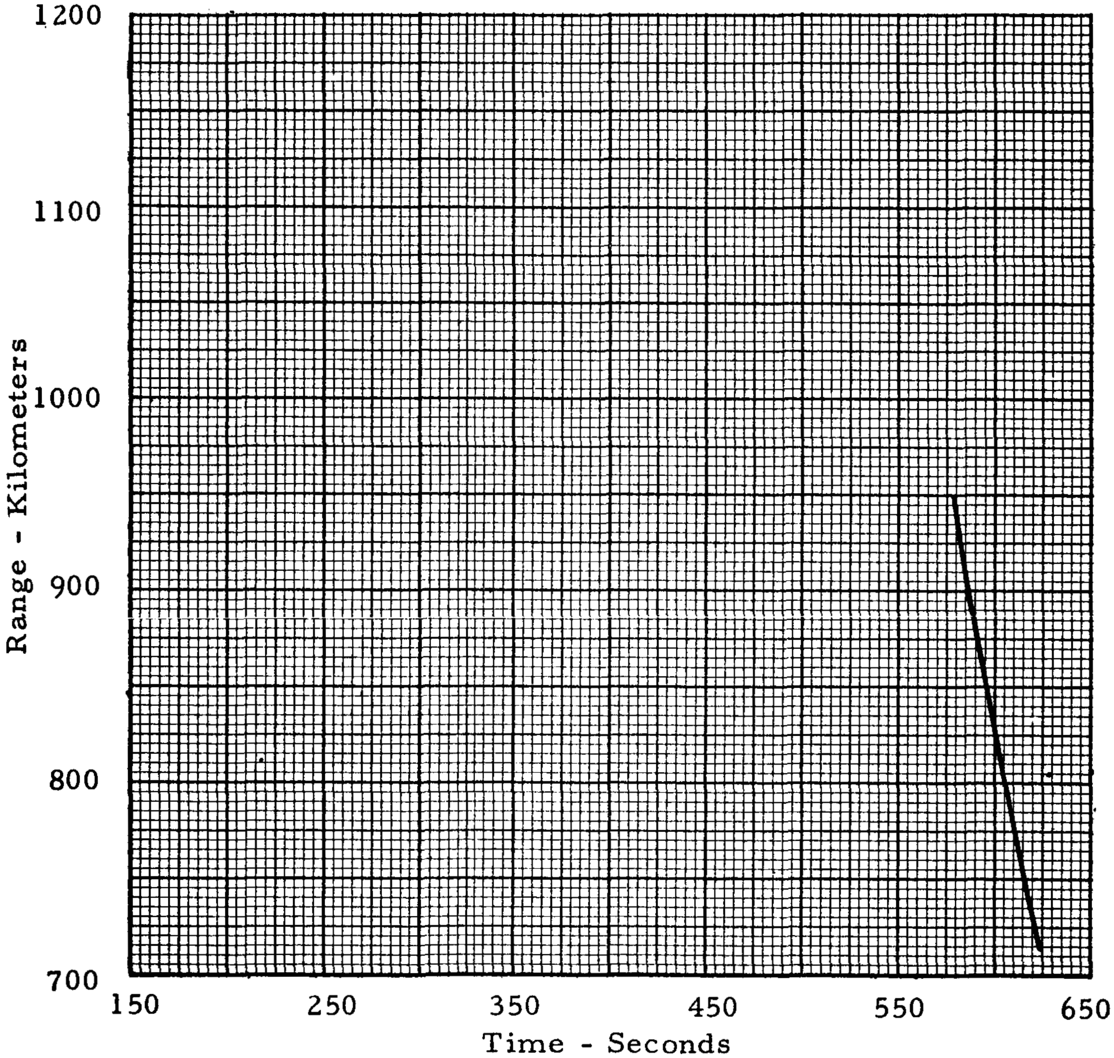

Figure 12

Range Rate As Seen From Cape Canaveral
105 NM Orbit Launch Phase,
Initial Bearing 105 Degrees

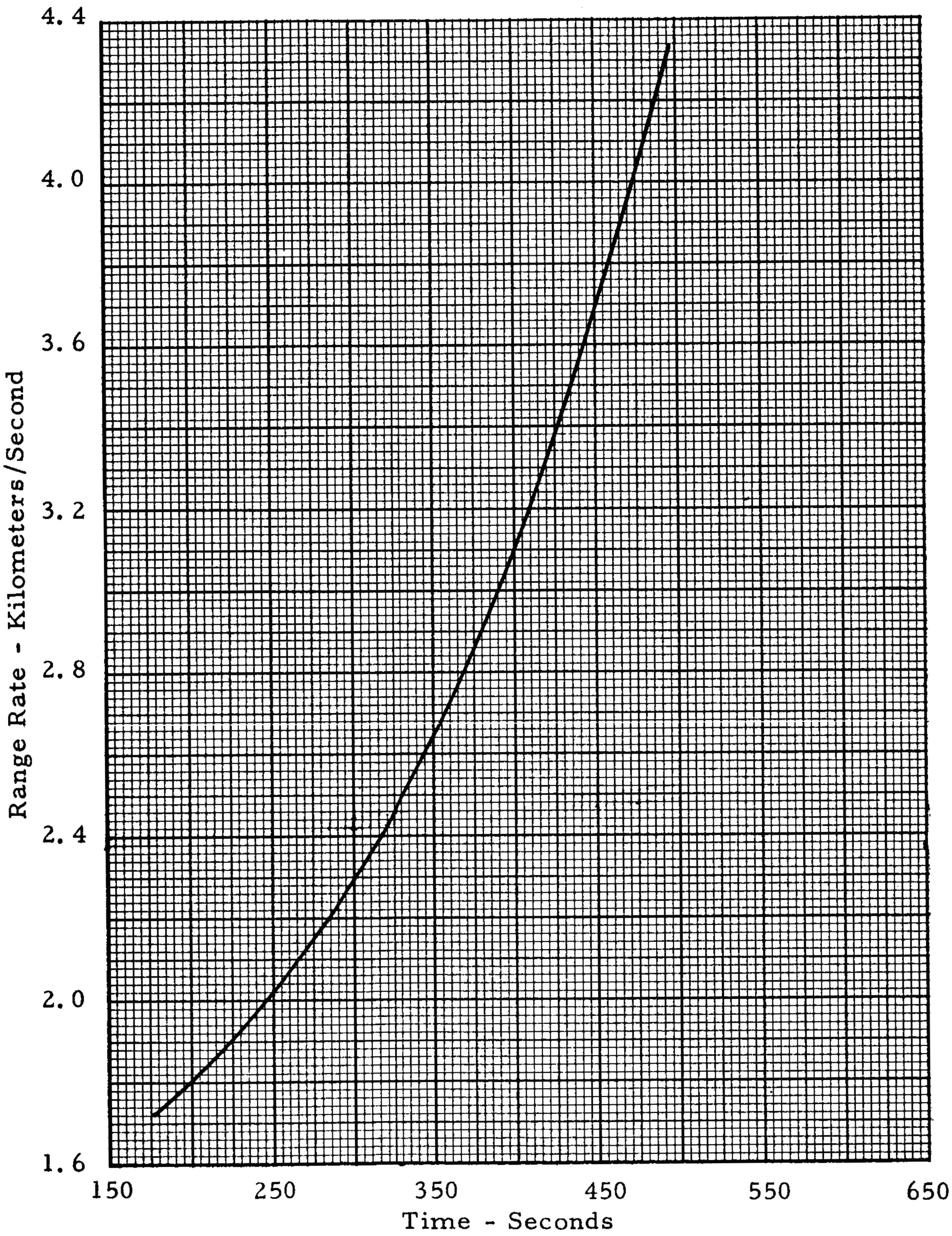

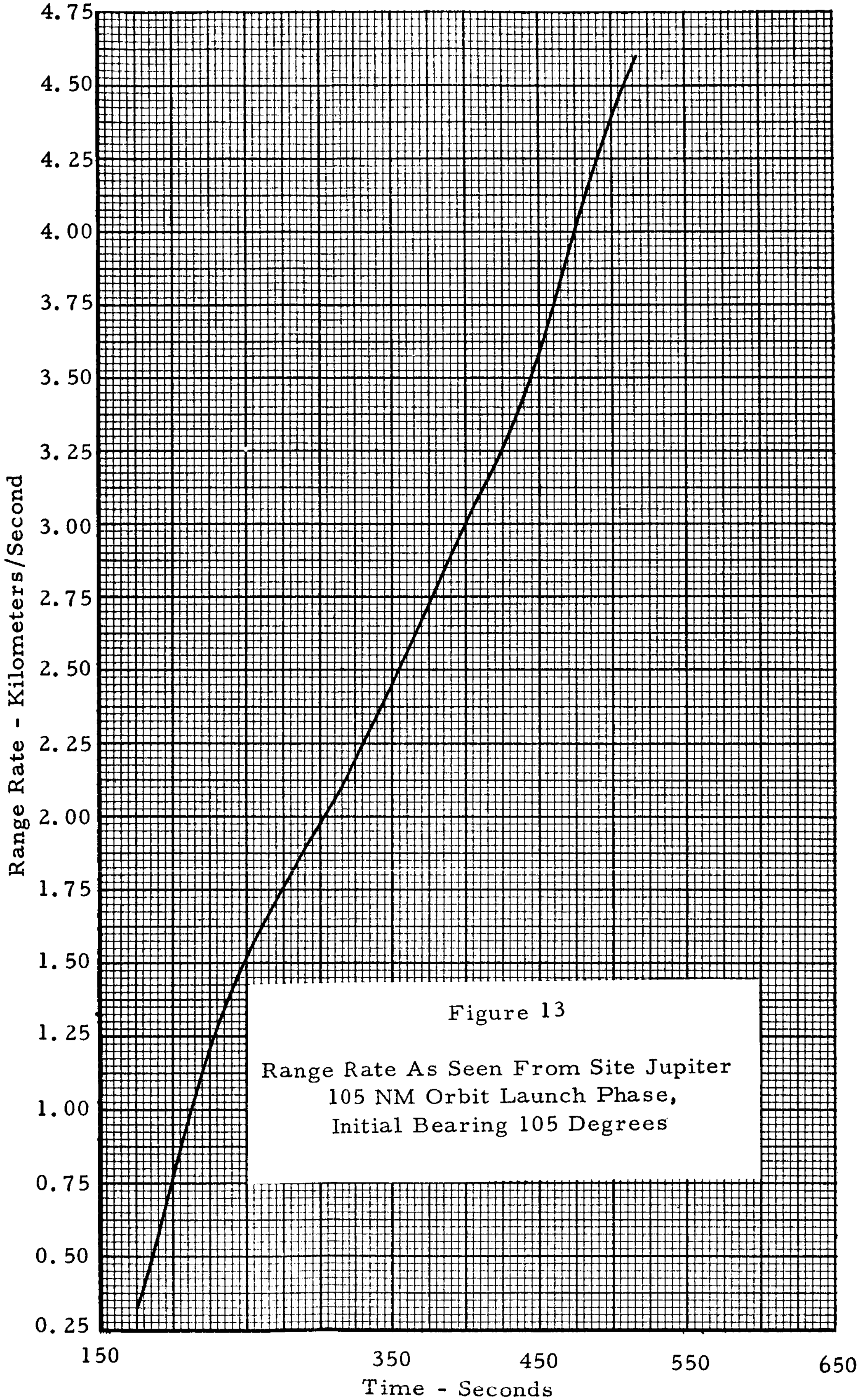

Figure 13

Range Rate As Seen From Site Jupiter
105 NM Orbit Launch Phase,
Initial Bearing 105 Degrees

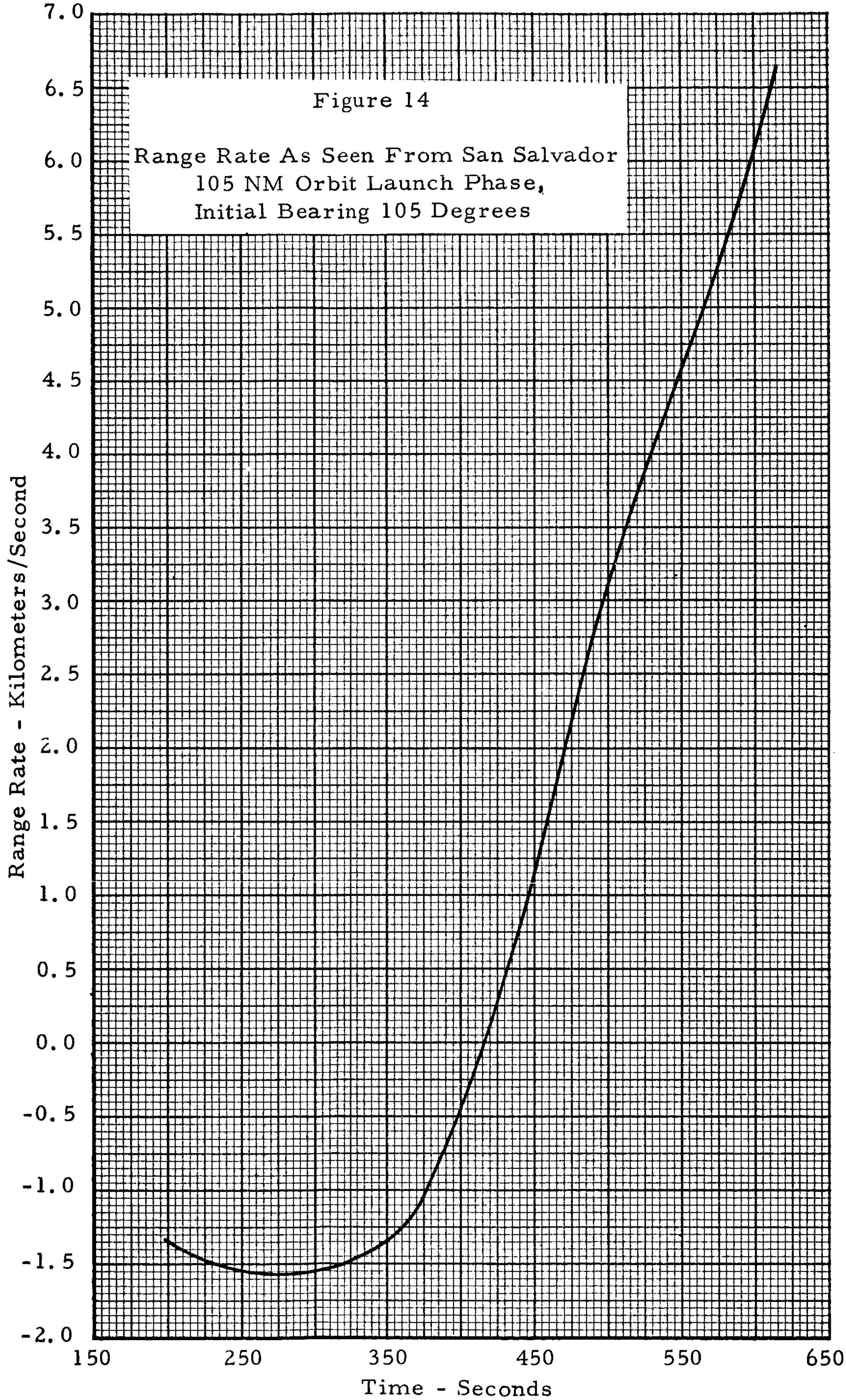
Figure 14
Range Rate As Seen From San Salvador
105 NM Orbit Launch Phase,
Initial Bearing 105 Degrees
Range Rate - Kilometers/Second
7.0
6.5
6.0
5.5
5.0
4.5
4.0
3.5
3.0
2.5
2.0
1.5
1.0
0.5
0.0
-0.5
-1.0
-1.5
-2.0
150
250
350
450
550
650
Time - Seconds

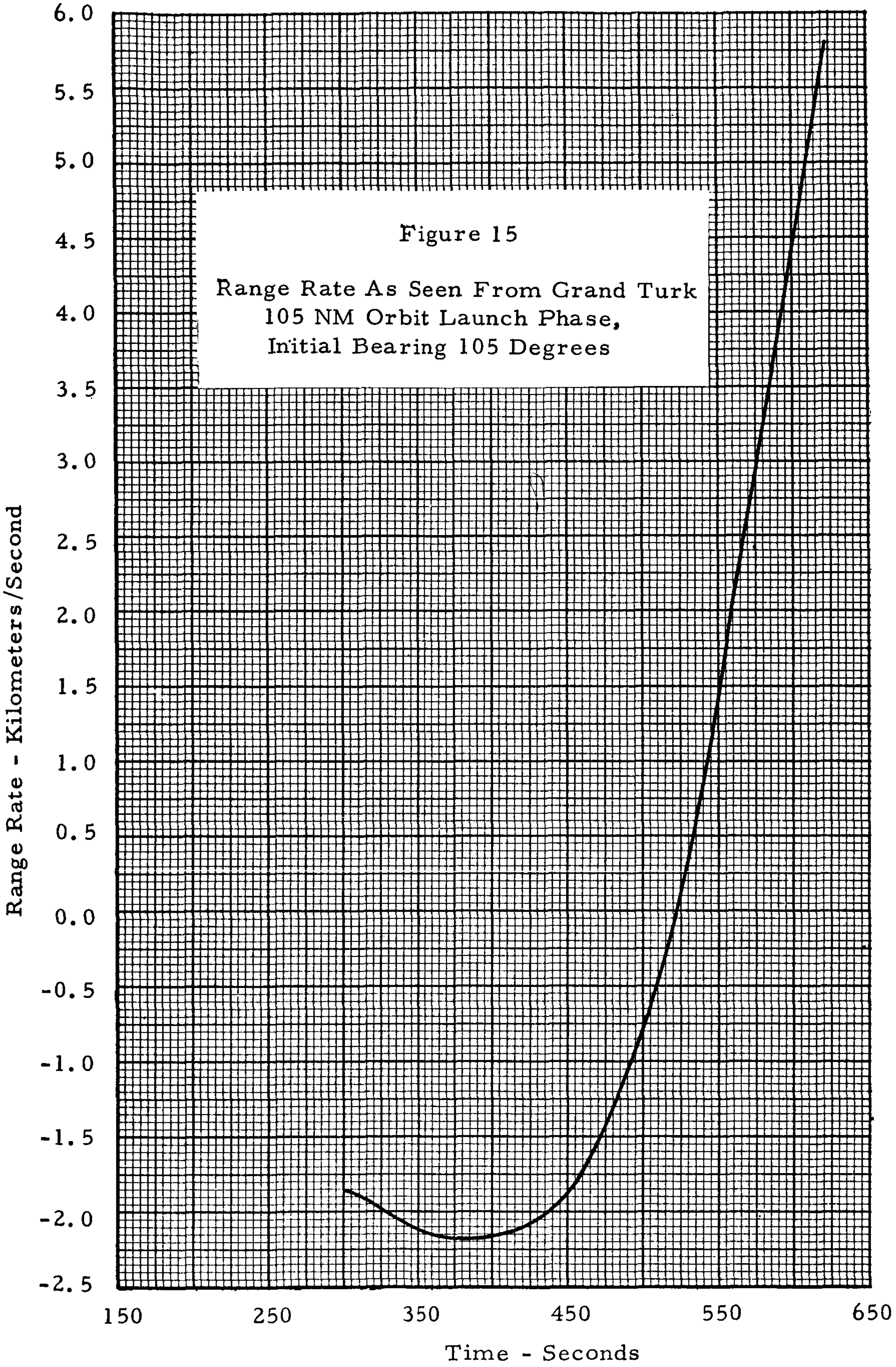

Figure 15

Range Rate As Seen From Grand Turk
105 NM Orbit Launch Phase,
Initial Bearing 105 Degrees

Figure 16

Range Rate As Seen From Bermuda
105 NM Orbit Launch Phase,
Initial Bearing 105 Degrees

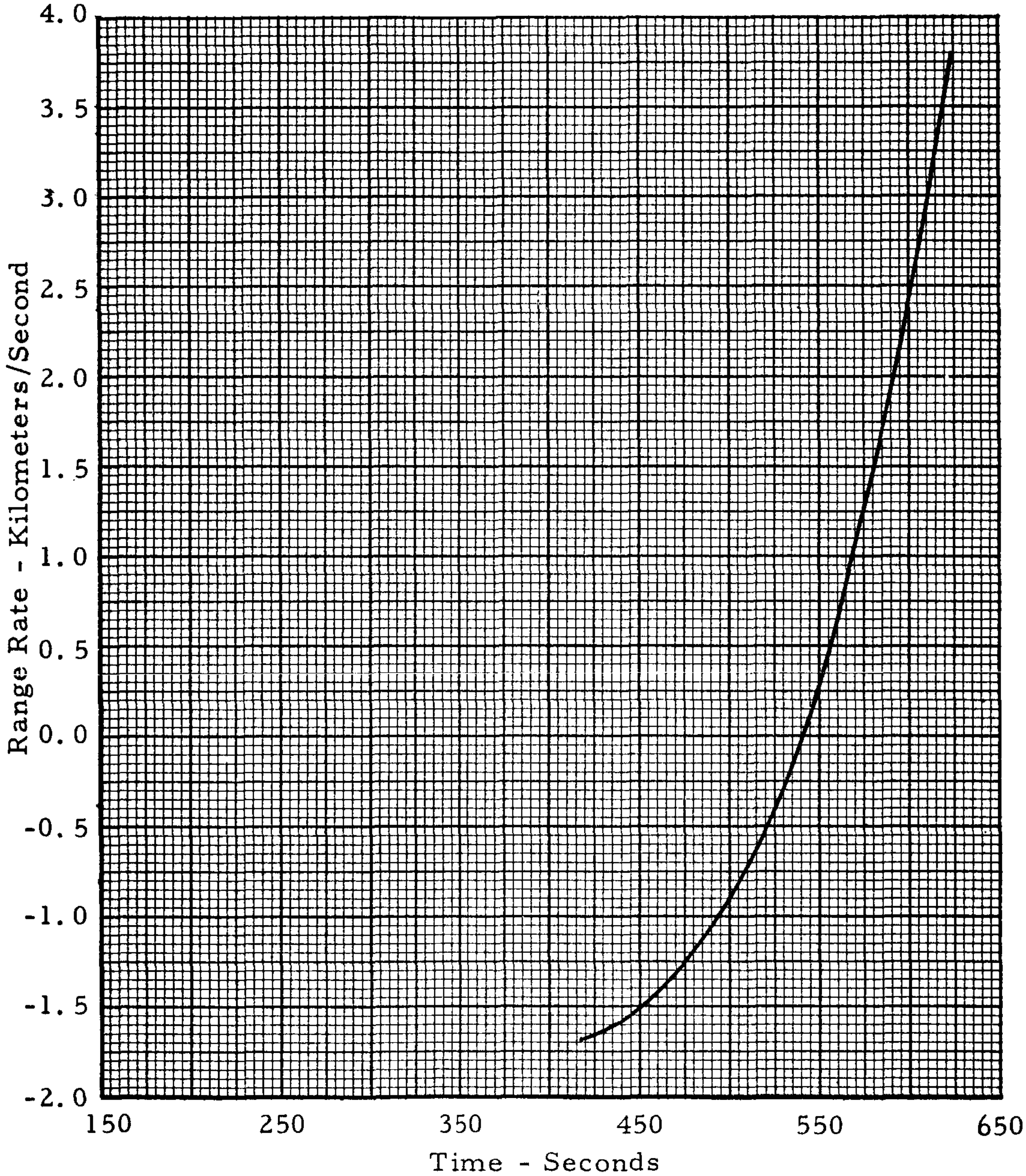

Figure 17

Range Rate As Seen From Antigua
105 NM Orbit Launch Phase,
Initial Bearing 105 Degrees

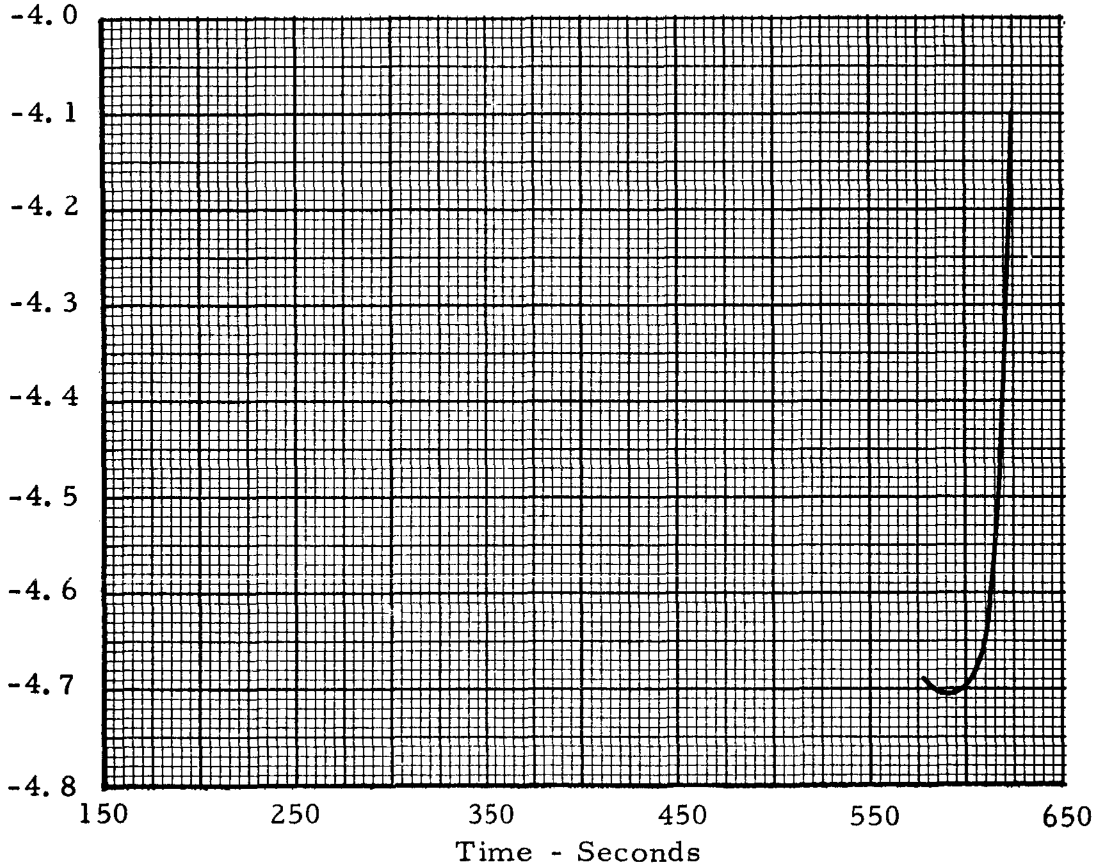

Figure 18

Absolute Value of Elevation Angle
As Seen From Cape Canaveral
105 NM Orbit Launch Phase,
Initial Bearing 105 Degrees

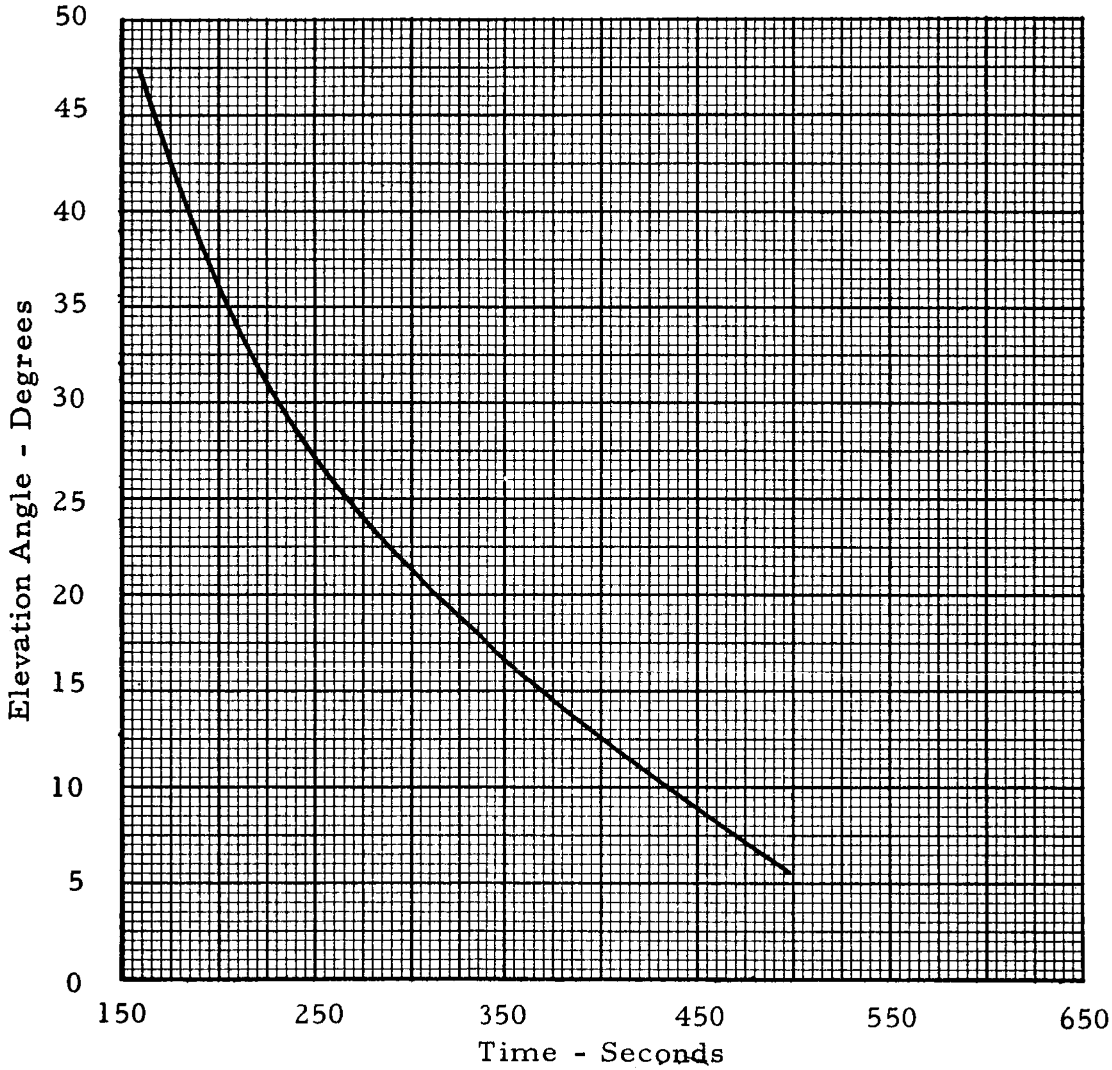

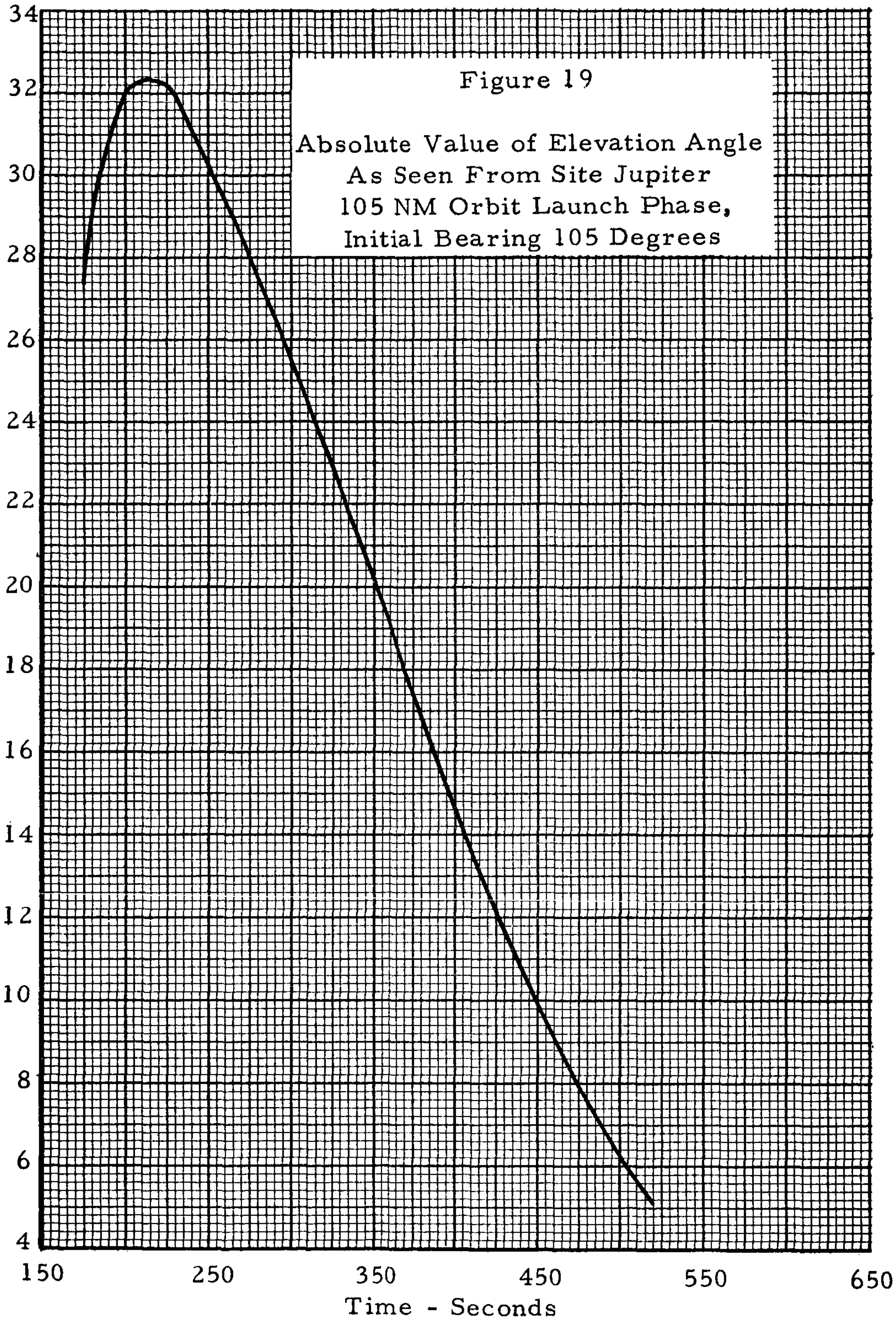

Figure 19
Absolute Value of Elevation Angle
As Seen From Site Jupiter
105 NM Orbit Launch Phase,
Initial Bearing 105 Degrees
34
32
30
28
26
24
22
20
18
16
14
12
10
8
6
4
150
250
350
450
550
650
Time - Seconds

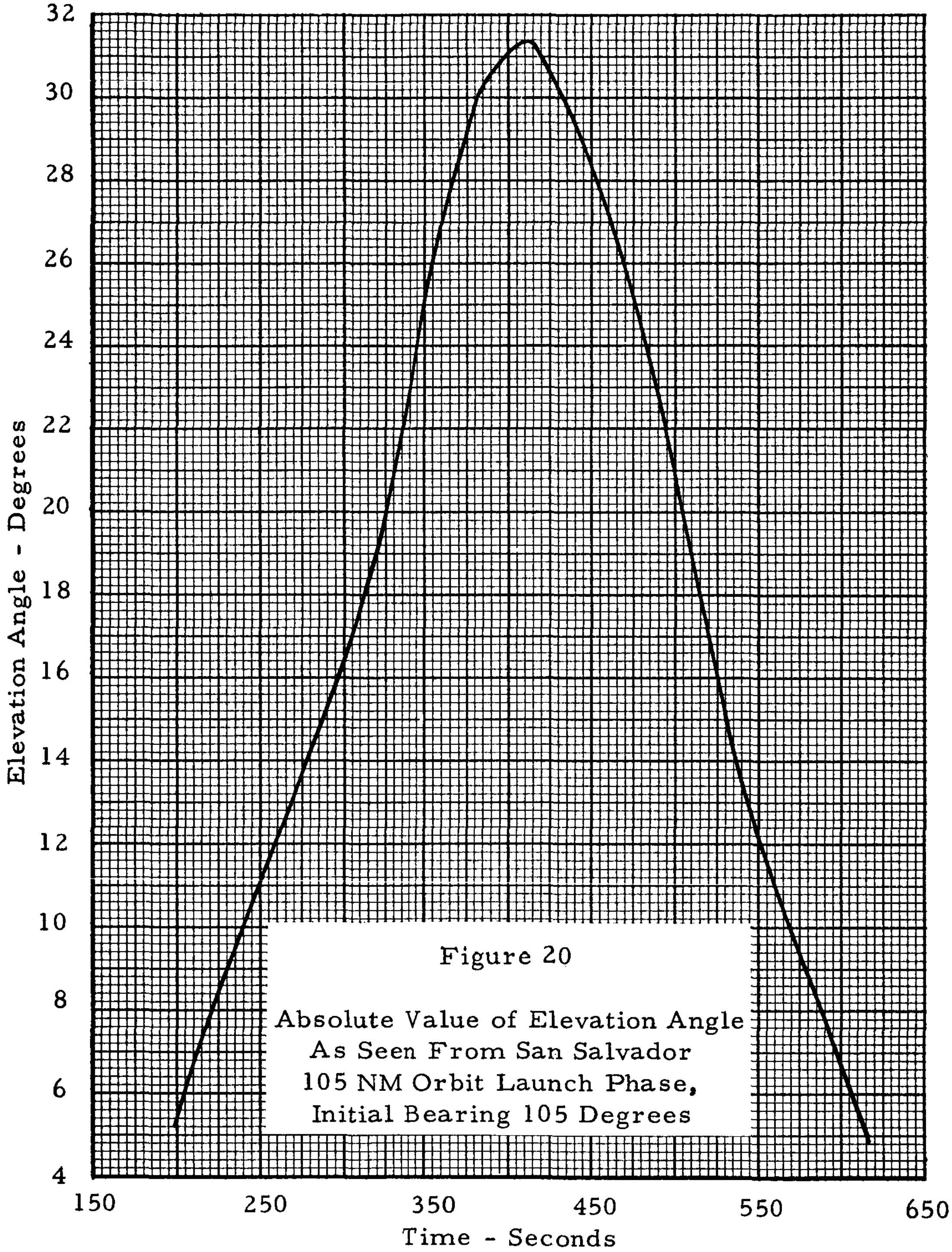

Figure 20

Absolute Value of Elevation Angle
As Seen From San Salvador
105 NM Orbit Launch Phase,
Initial Bearing 105 Degrees

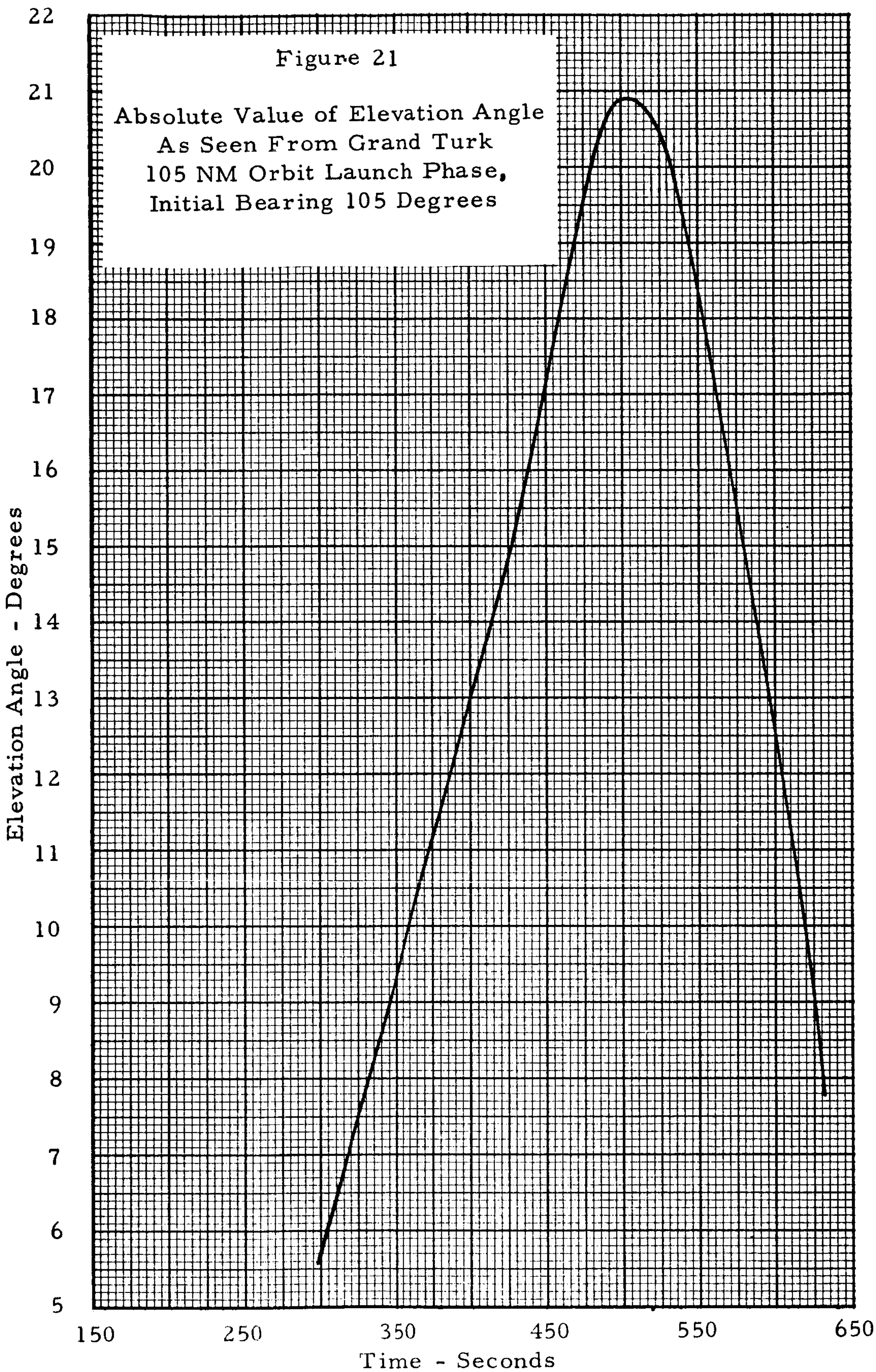
Figure 21
Absolute Value of Elevation Angle
As Seen From Grand Turk
105 NM Orbit Launch Phase,
Initial Bearing 105 Degrees
Elevation Angle - Degrees
22
21
20
19
18
17
16
15
14
13
12
11
10
9
8
7
6
5
150
250
350
450
550
650
Time - Seconds

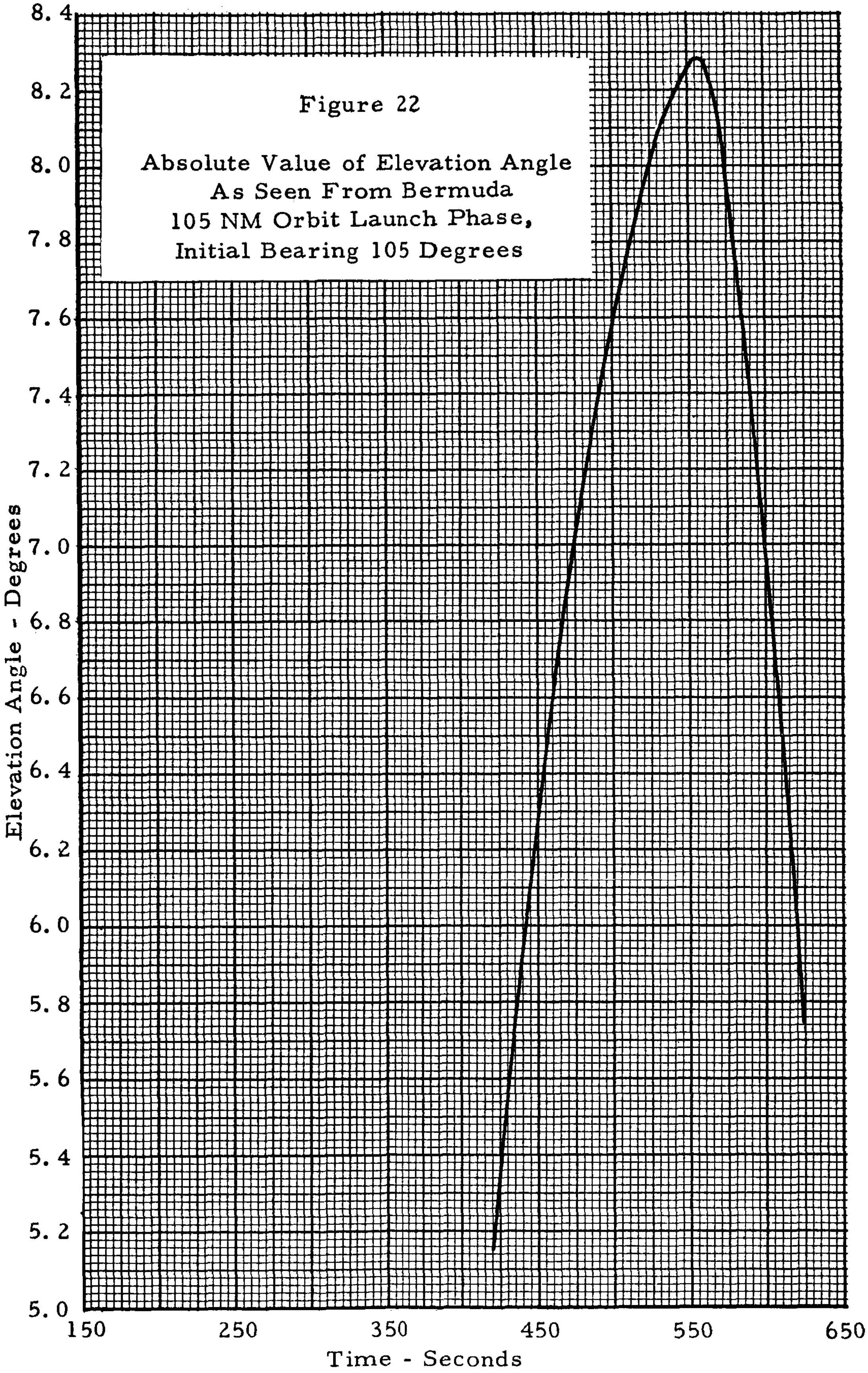
Figure 22
Absolute Value of Elevation Angle
As Seen From Bermuda
105 NM Orbit Launch Phase,
Initial Bearing 105 Degrees
8.4
8.2
8.0
7.8
7.6
7.4
7.2
7.0
6.8
6.6
6.4
6.2
6.0
5.8
5.6
5.4
5.2
5.0
Elevation Angle - Degrees
150
250
350
450
550
650
Time - Seconds

Figure 23

Absolute Value of Elevation Angle
As Seen From Antigua
105 NM Orbit Launch Phase,
Initial Bearing 105 Degrees

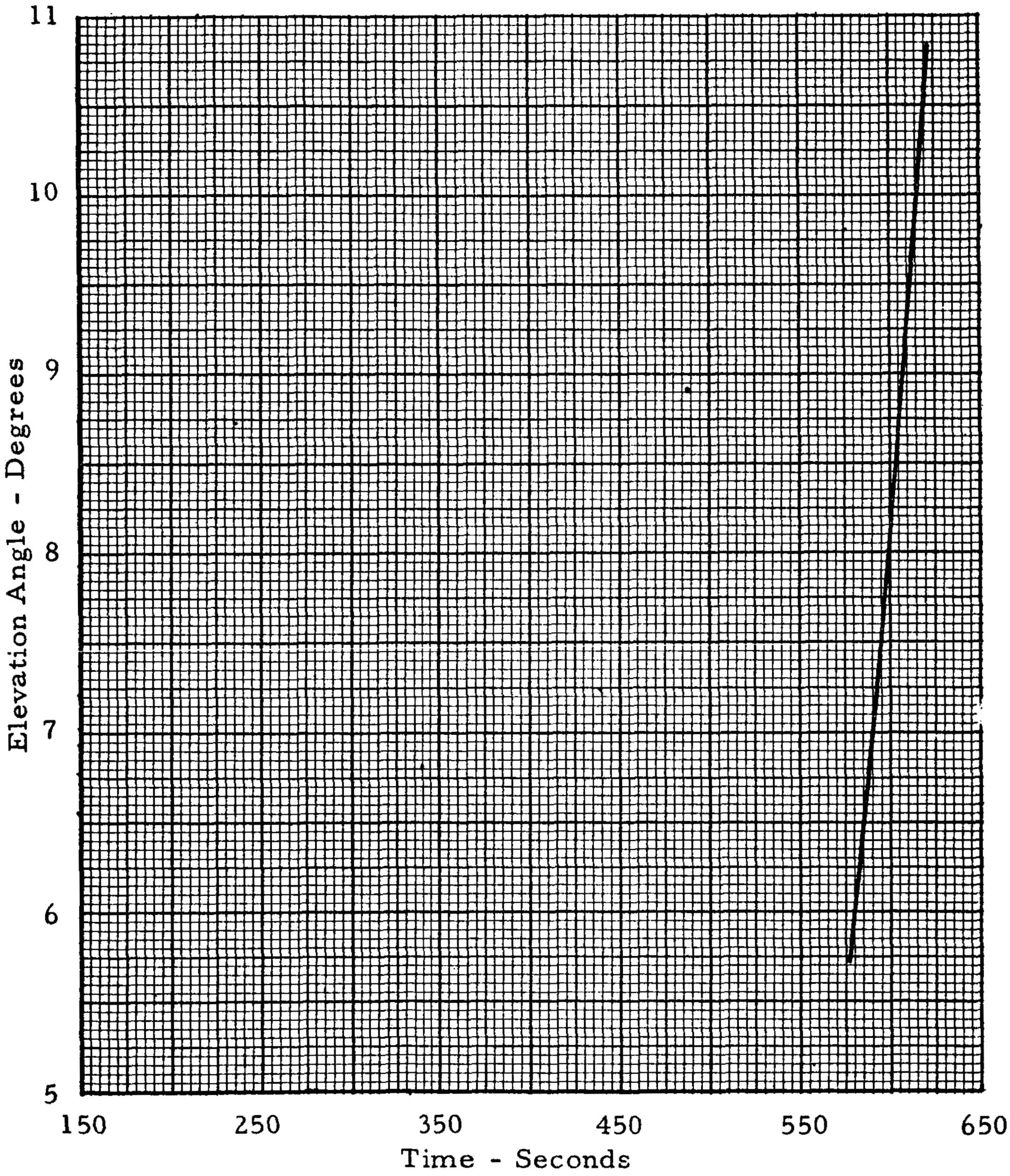

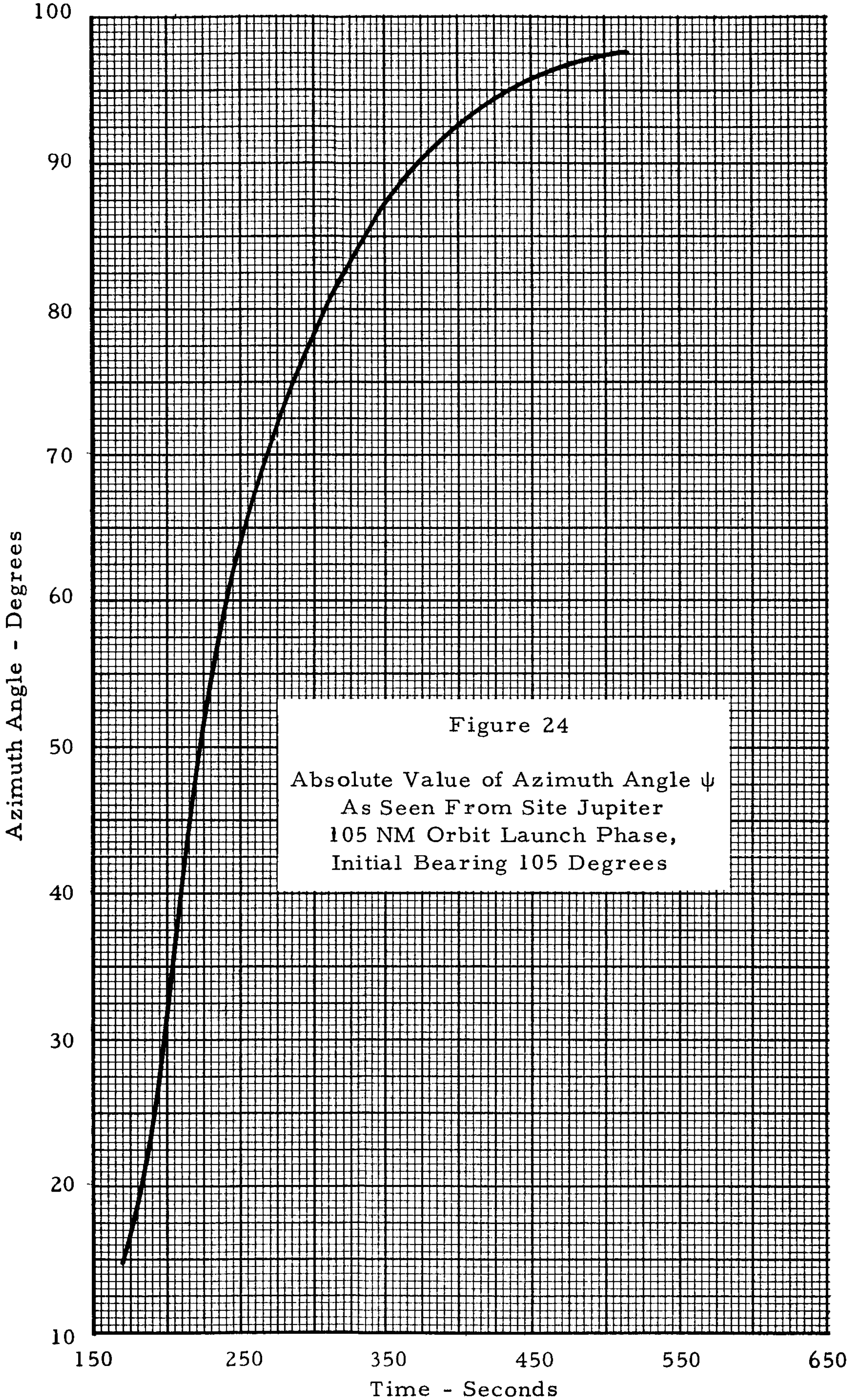

Figure 24

Absolute Value of Azimuth Angle ψ
As Seen From Site Jupiter
105 NM Orbit Launch Phase,
Initial Bearing 105 Degrees

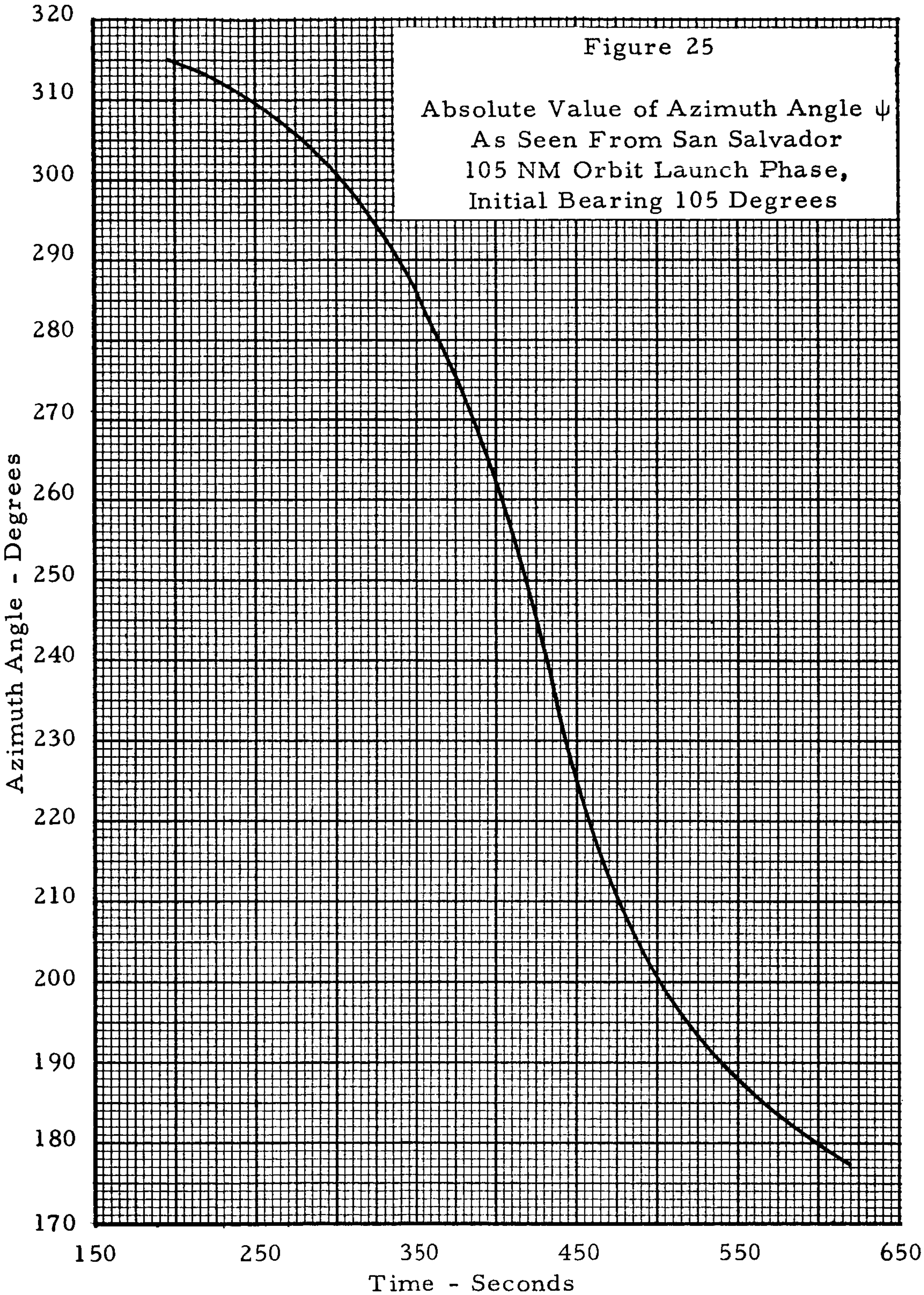
Figure 25
Absolute Value of Azimuth Angle ψ
As Seen From San Salvador
105 NM Orbit Launch Phase,
Initial Bearing 105 Degrees
320
310
300
290
280
270
260
250
240
230
220
210
200
190
180
170
150
250
350
450
550
650
Azimuth Angle - Degrees
Time - Seconds

Figure 26

Absolute Value of Azimuth Angle ψ
As Seen From Grand Turk
105 NM Orbit Launch Phase,
Initial Bearing 105 Degrees

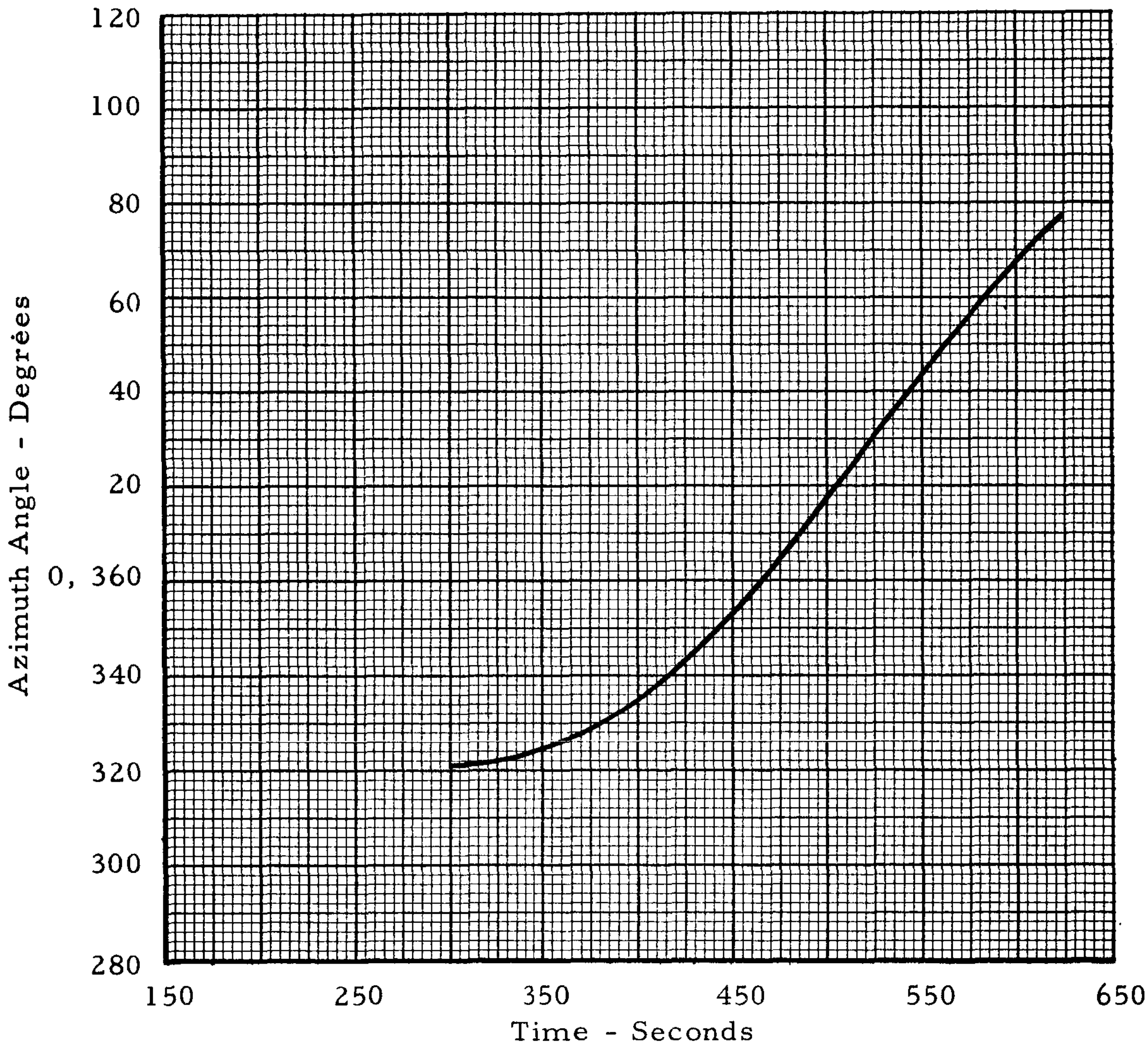

Figure 27

Absolute Value of Azimuth Angle ψ
As Seen From Bermuda
105 NM Orbit Launch Phase
Initial Bearing 105 Degrees

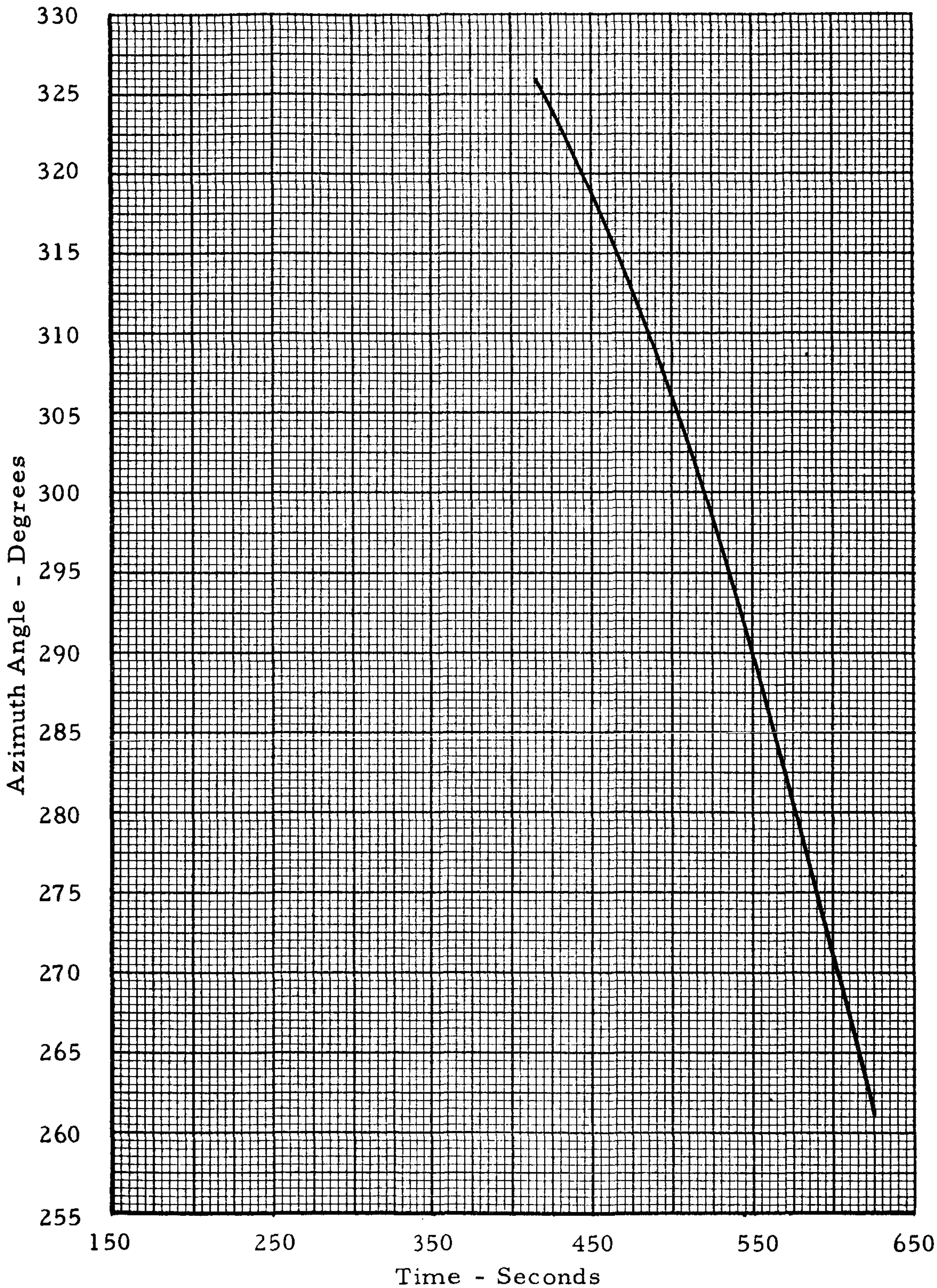

Figure 28

Absolute Value of Azimuth Angle ψ
As Seen From Antigua
105 NM Orbit Launch Phase,
Initial Bearing 105 Degrees

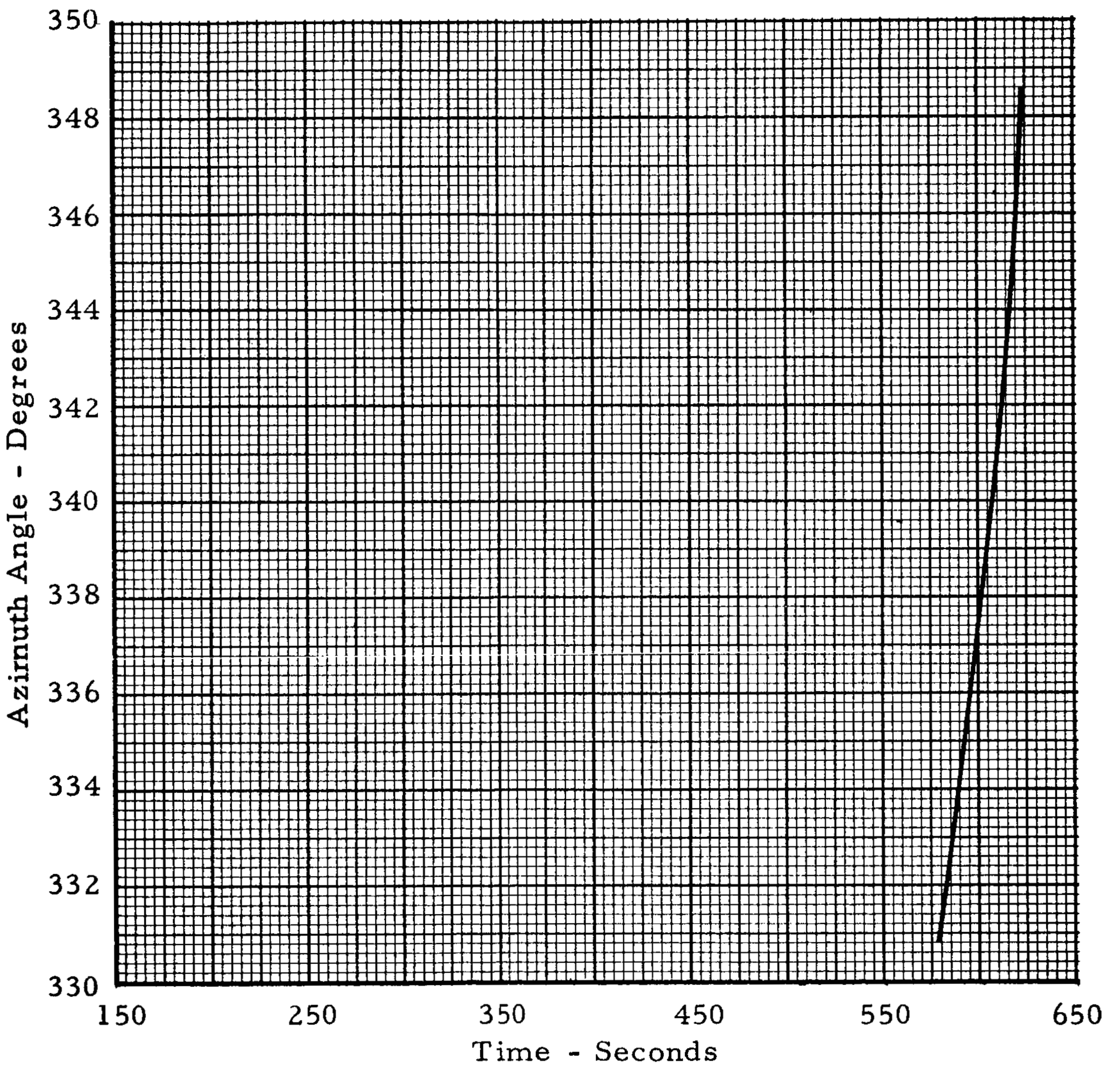

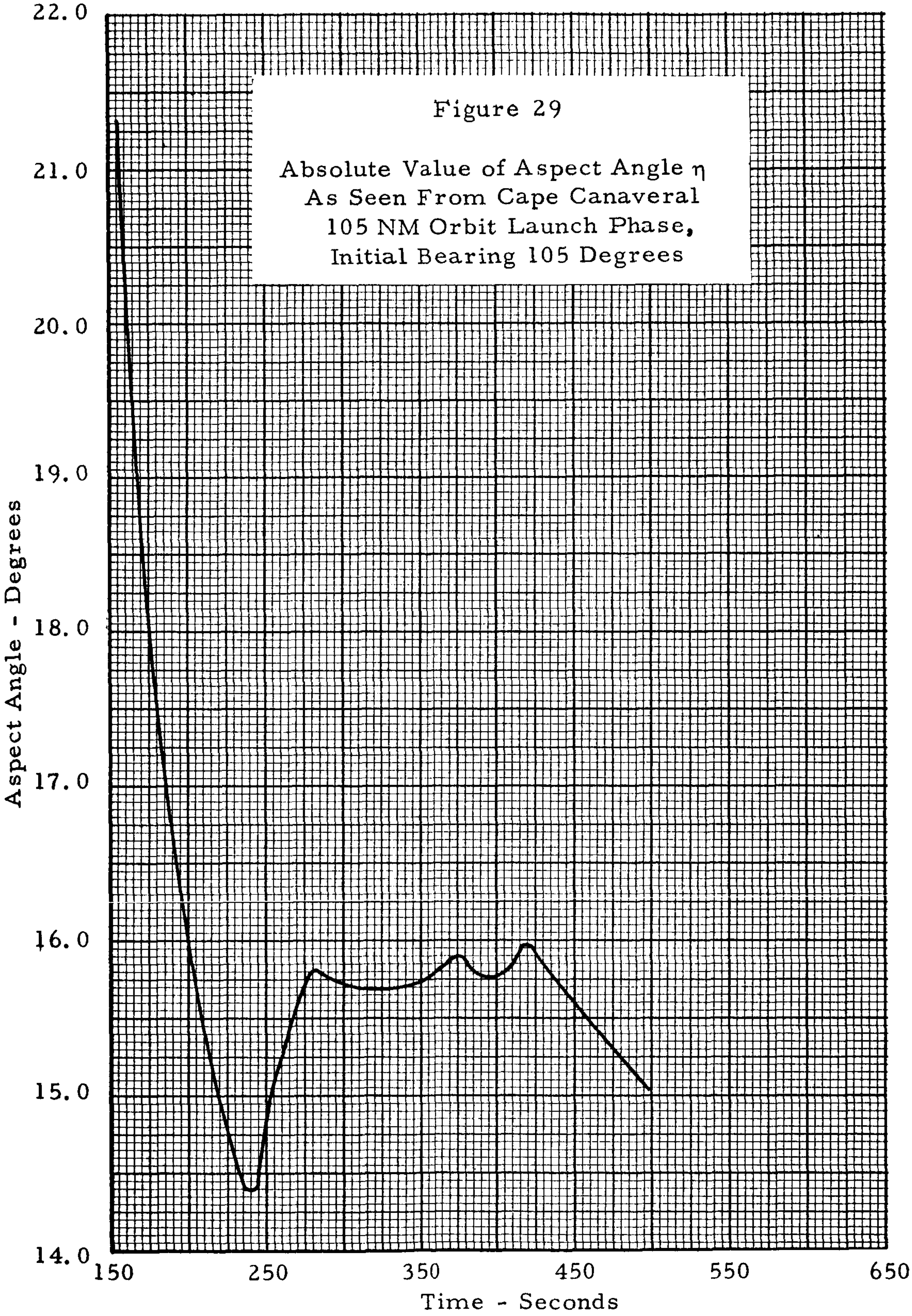
Figure 29
Absolute Value of Aspect Angle η
As Seen From Cape Canaveral
105 NM Orbit Launch Phase,
Initial Bearing 105 Degrees
22.0
21.0
20.0
19.0
18.0
17.0
16.0
15.0
14.0
Aspect Angle - Degrees
150
250
350
450
550
650
Time - Seconds

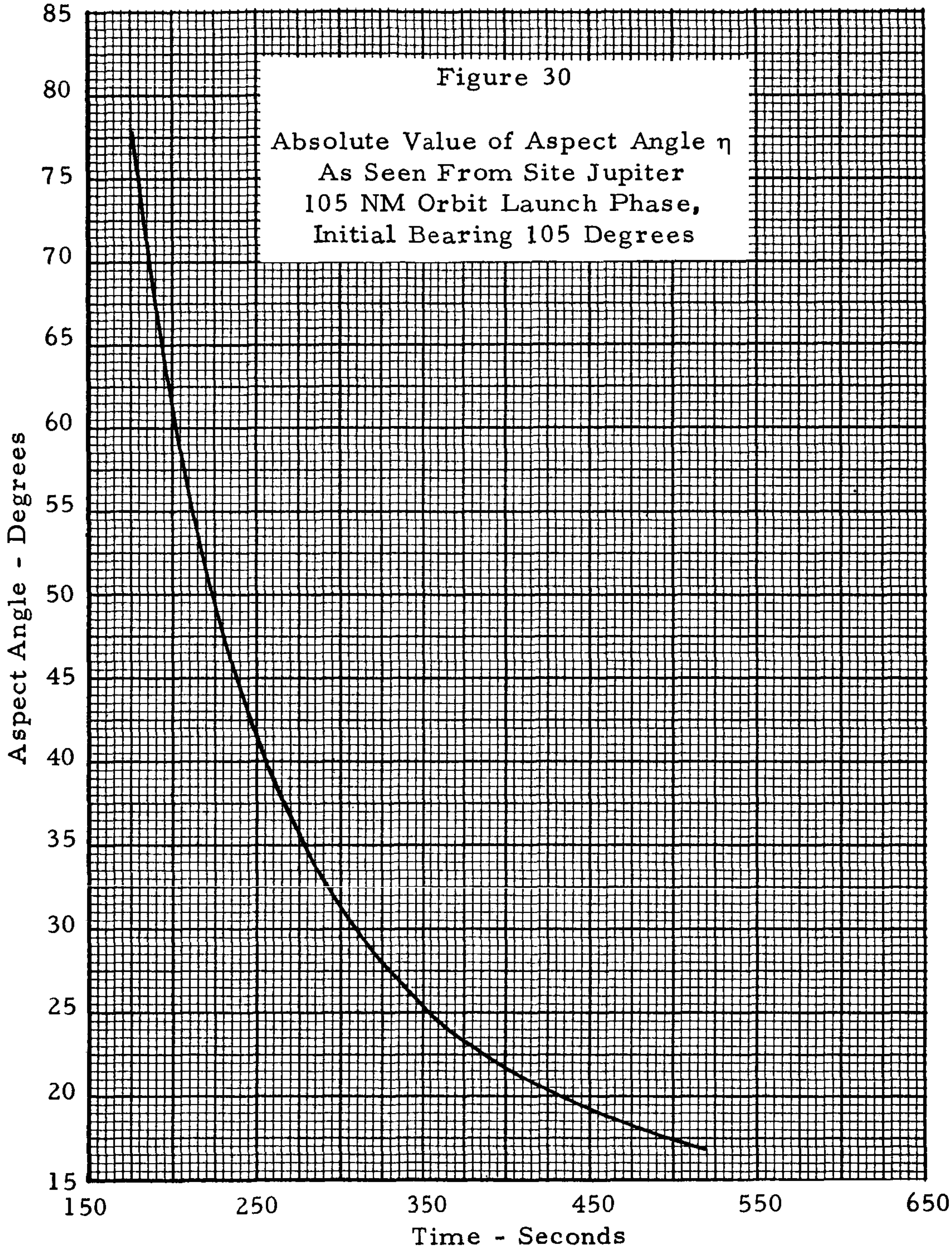

Figure 30
Absolute Value of Aspect Angle η
As Seen From Site Jupiter
105 NM Orbit Launch Phase,
Initial Bearing 105 Degrees
85
80
75
70
65
60
55
50
45
40
35
30
25
20
15
Aspect Angle - Degrees
150
250
350
450
550
650
Time - Seconds

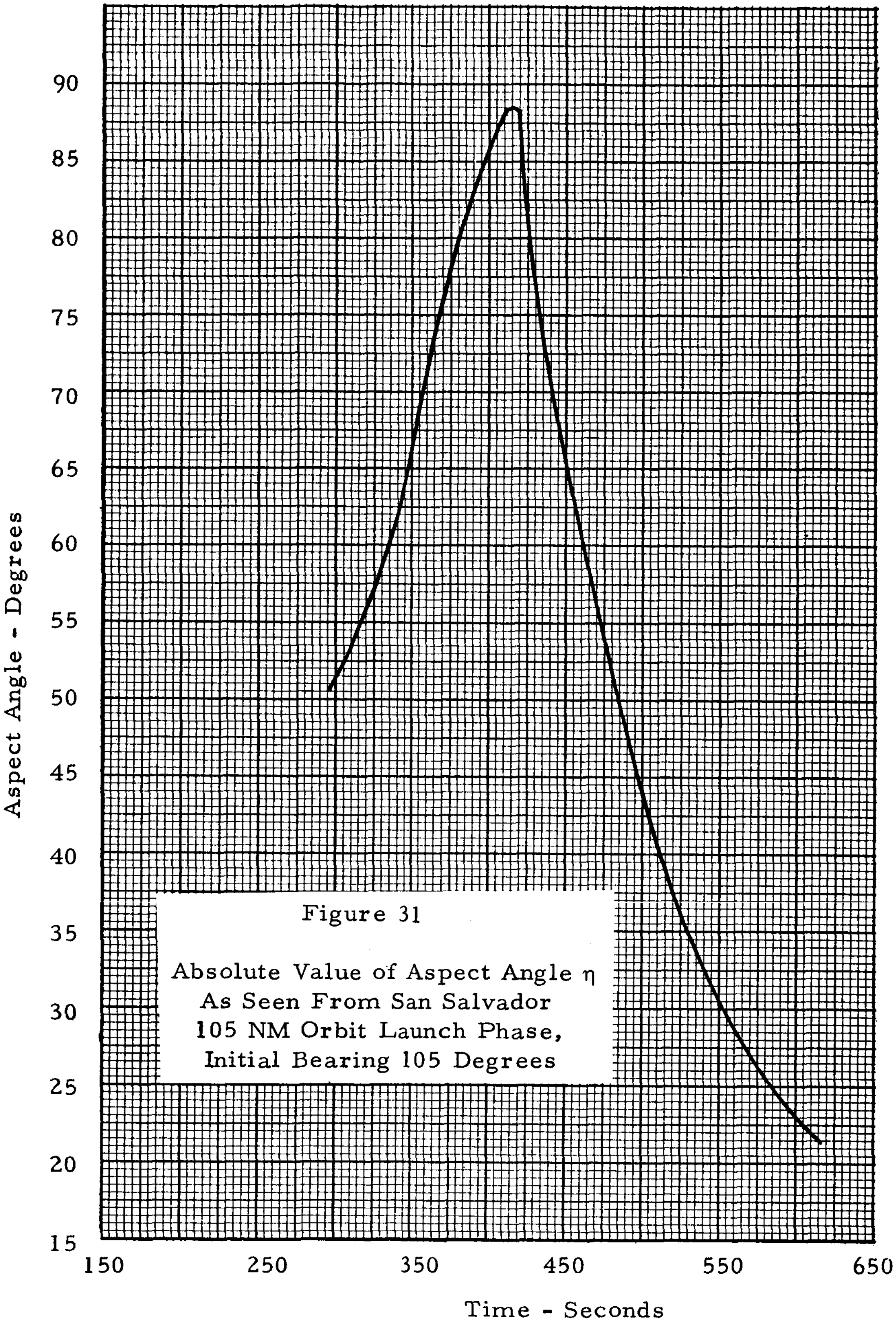

Figure 31

Absolute Value of Aspect Angle η
As Seen From San Salvador
105 NM Orbit Launch Phase,
Initial Bearing 105 Degrees

Figure 32

Absolute Value of Aspect Angle η
As Seen From Grand Turk
105 NM Orbit Launch Phase,
Initial Bearing 105 Degrees

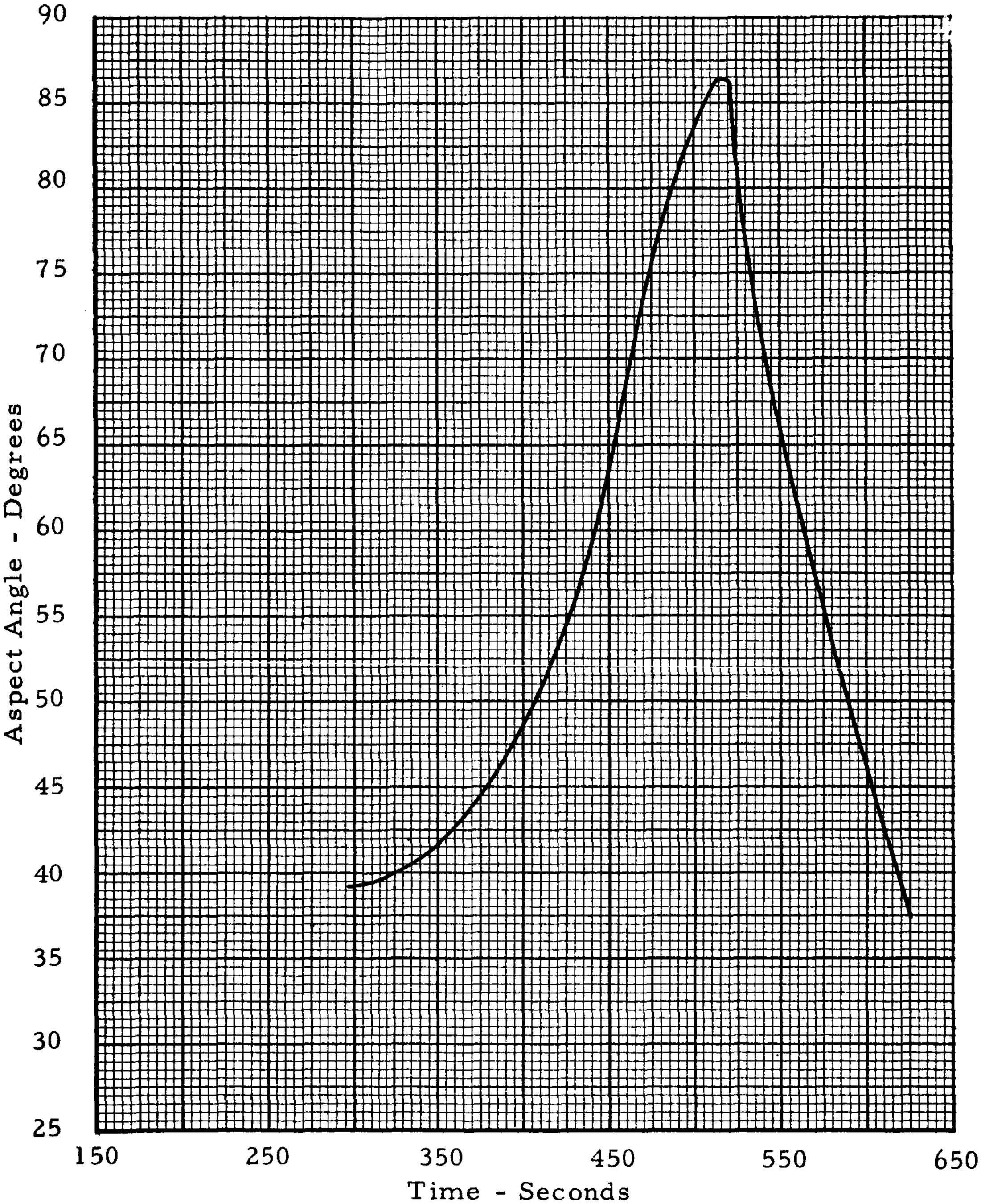

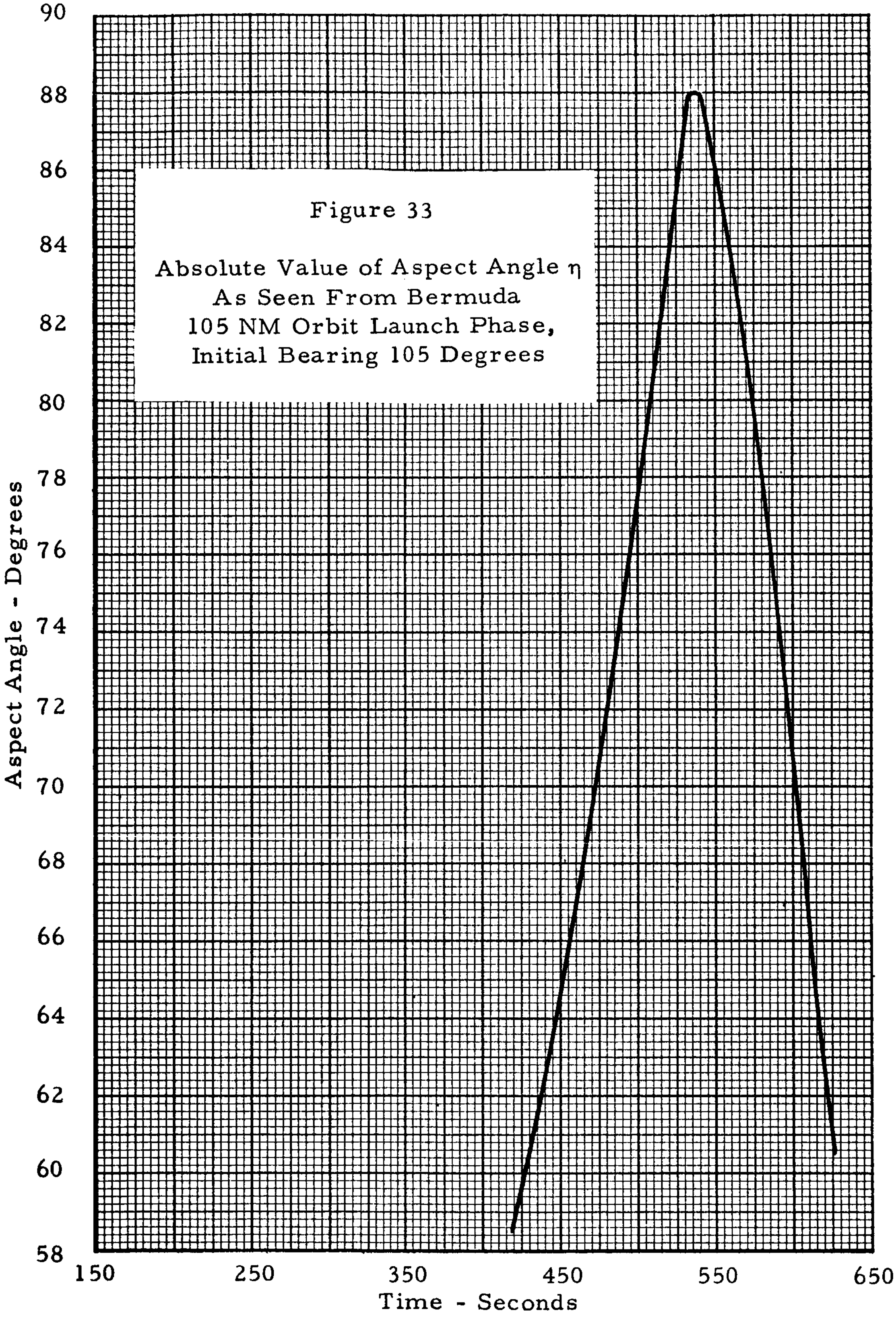

Figure 33

Absolute Value of Aspect Angle η
As Seen From Bermuda
105 NM Orbit Launch Phase,
Initial Bearing 105 Degrees

Figure 34

Absolute Value of Aspect Angle η
As Seen From Antigua
105 NM Orbit Launch Phase,
Initial Bearing 105 Degrees

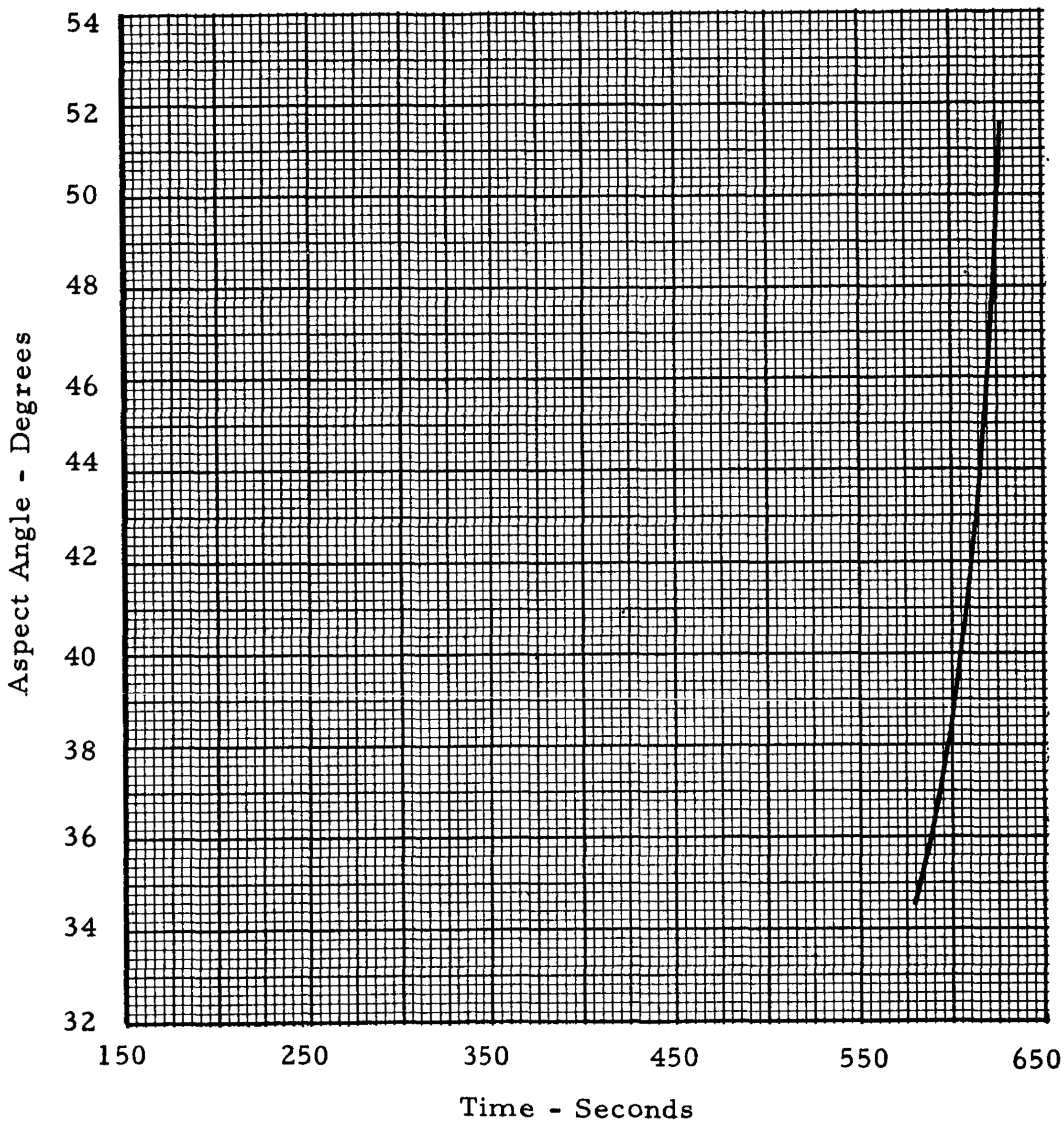

Figure 35

Absolute Value of
Vehicle Azimuth Angle
As Seen From Cape Canaveral
105 NM Orbit Launch Phase,
Initial Bearing 105 Degrees

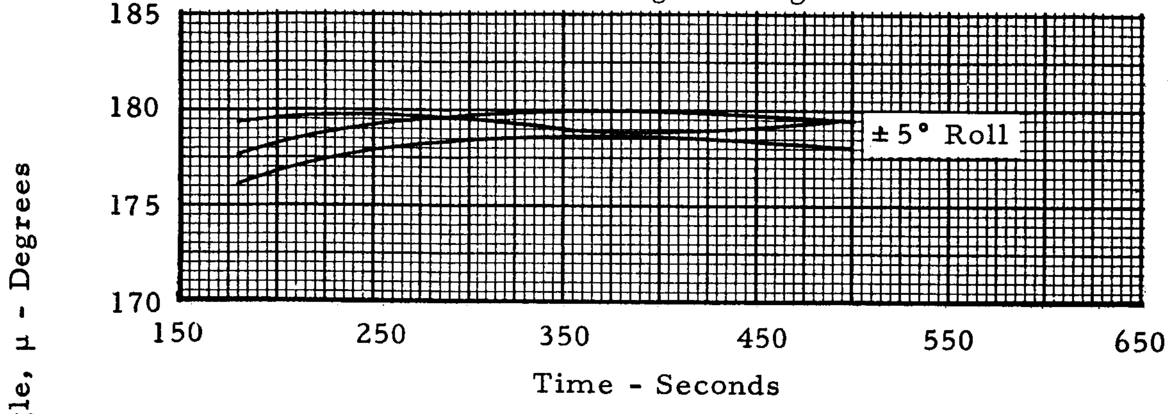

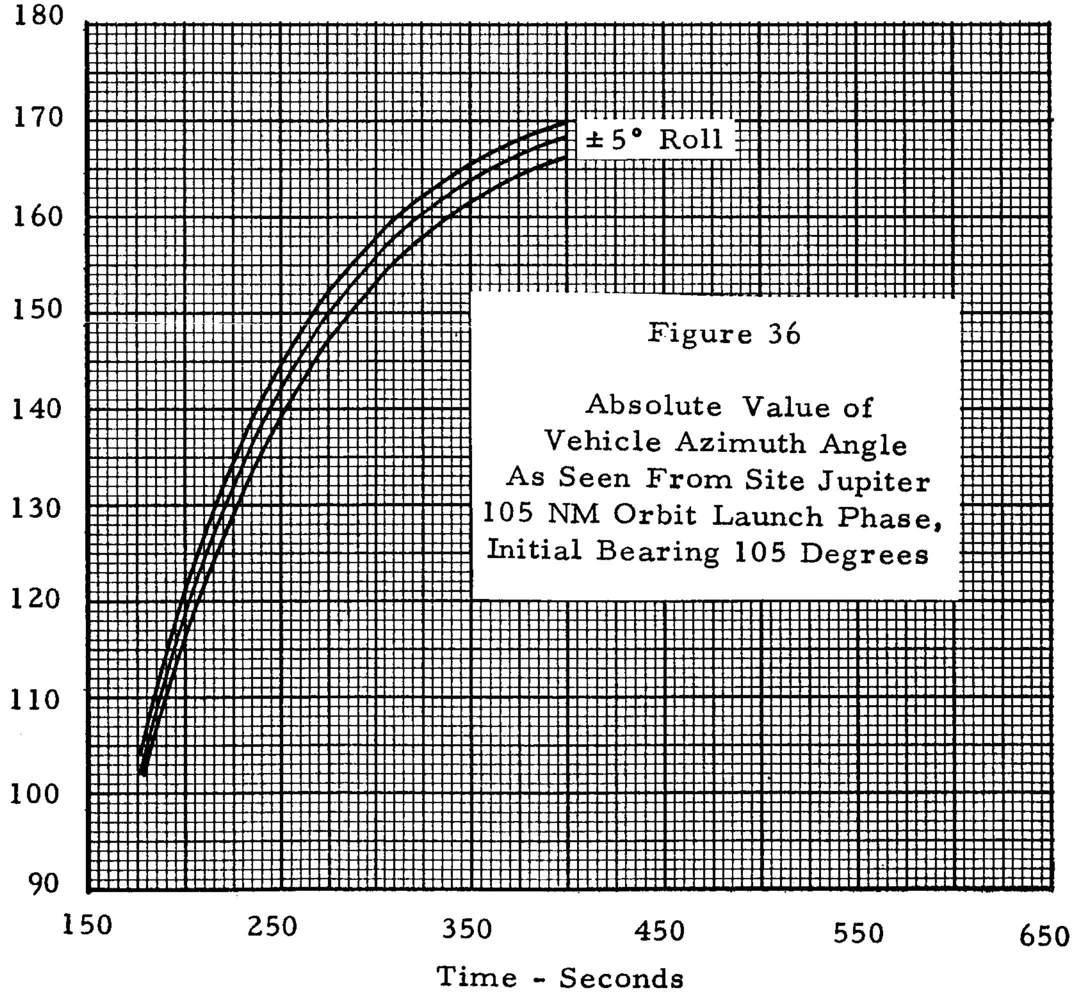

Figure 36

Absolute Value of
Vehicle Azimuth Angle
As Seen From Site Jupiter
105 NM Orbit Launch Phase,
Initial Bearing 105 Degrees

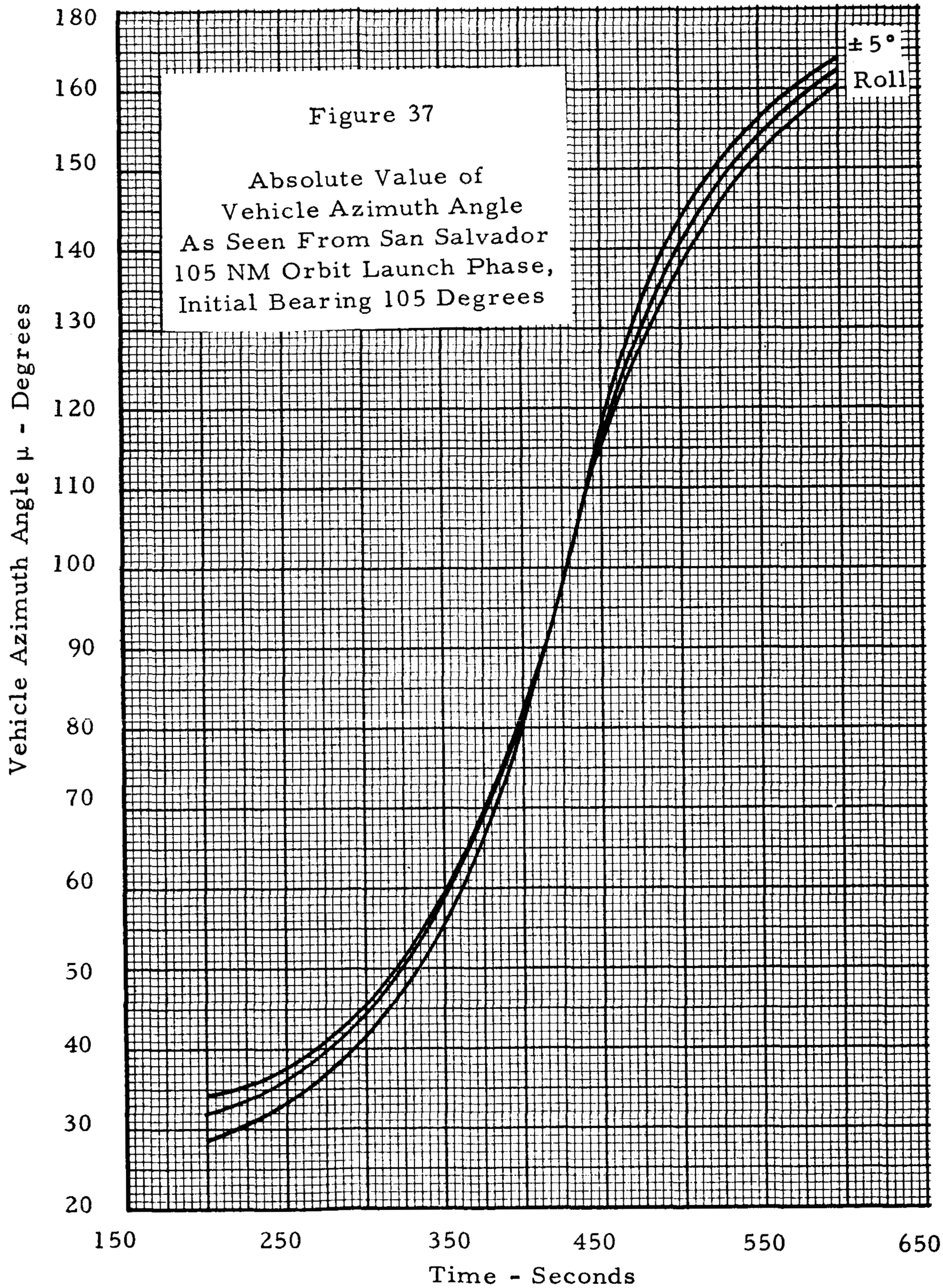
Figure 37
Absolute Value of
Vehicle Azimuth Angle
As Seen From San Salvador
105 NM Orbit Launch Phase,
Initial Bearing 105 Degrees
±5°
Roll
Vehicle Azimuth Angle μ - Degrees
180
160
150
140
130
120
110
100
90
80
70
60
50
40
30
20
150
250
350
450
550
650
Time - Seconds

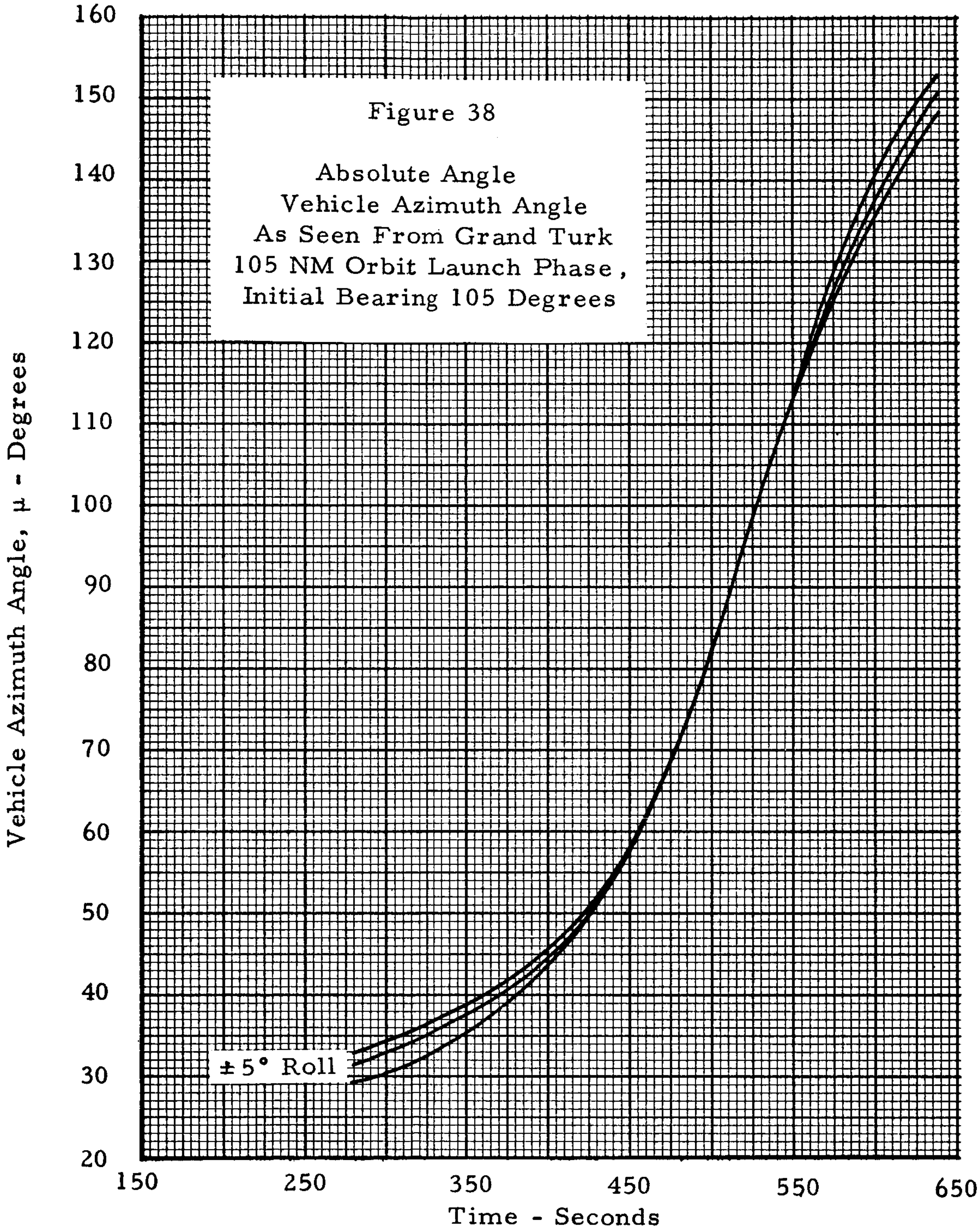
Figure 38
Absolute Angle
Vehicle Azimuth Angle
As Seen From Grand Turk
105 NM Orbit Launch Phase,
Initial Bearing 105 Degrees
±5° Roll
Vehicle Azimuth Angle, μ - Degrees
160
150
140
130
120
110
100
90
80
70
60
50
40
30
20
150
250
350
450
550
650
Time - Seconds

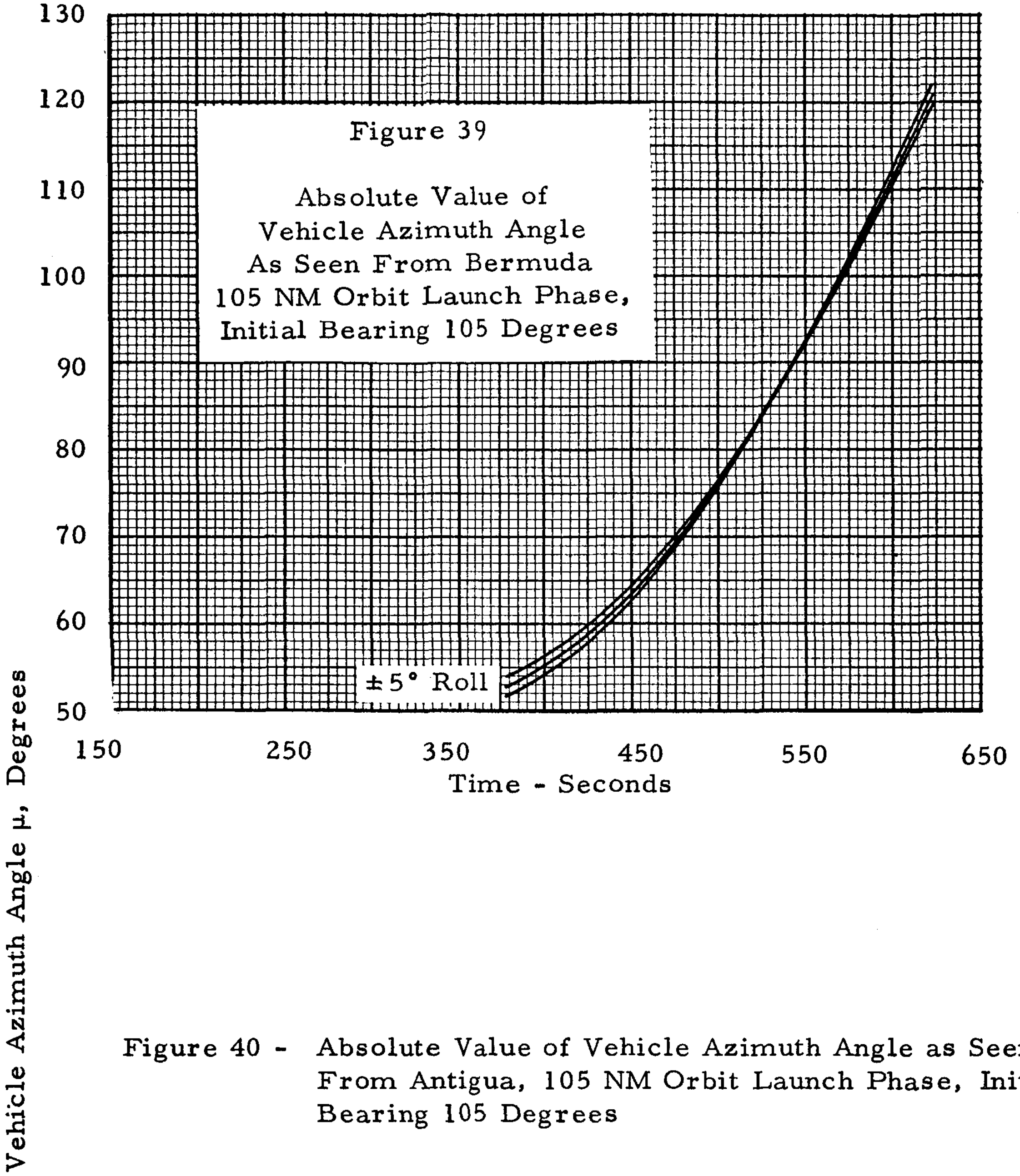

Figure 40 - Absolute Value of Vehicle Azimuth Angle as Seen From Antigua, 105 NM Orbit Launch Phase, Initial Bearing 105 Degrees

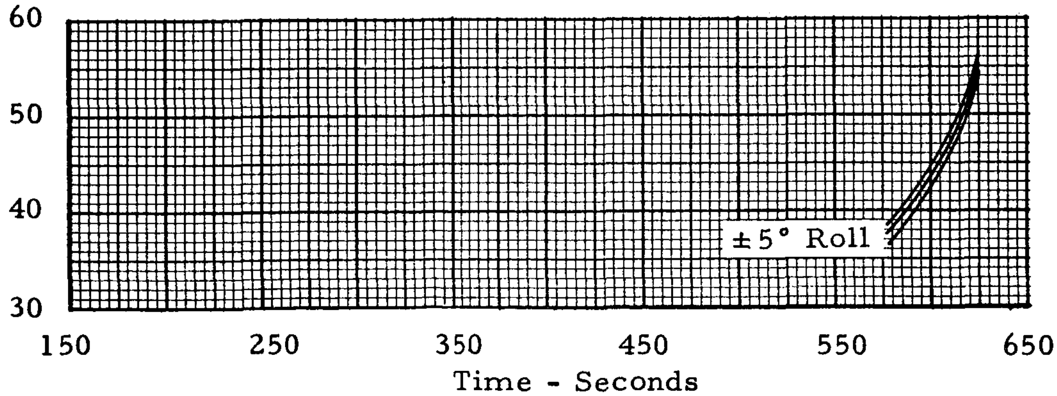

Figure 41

Absolute Value of Vehicle Elevation Angle
As Seen From Cape Canaveral, 105 NM Orbit Launch Phase,
Initial Bearing 105 Degrees

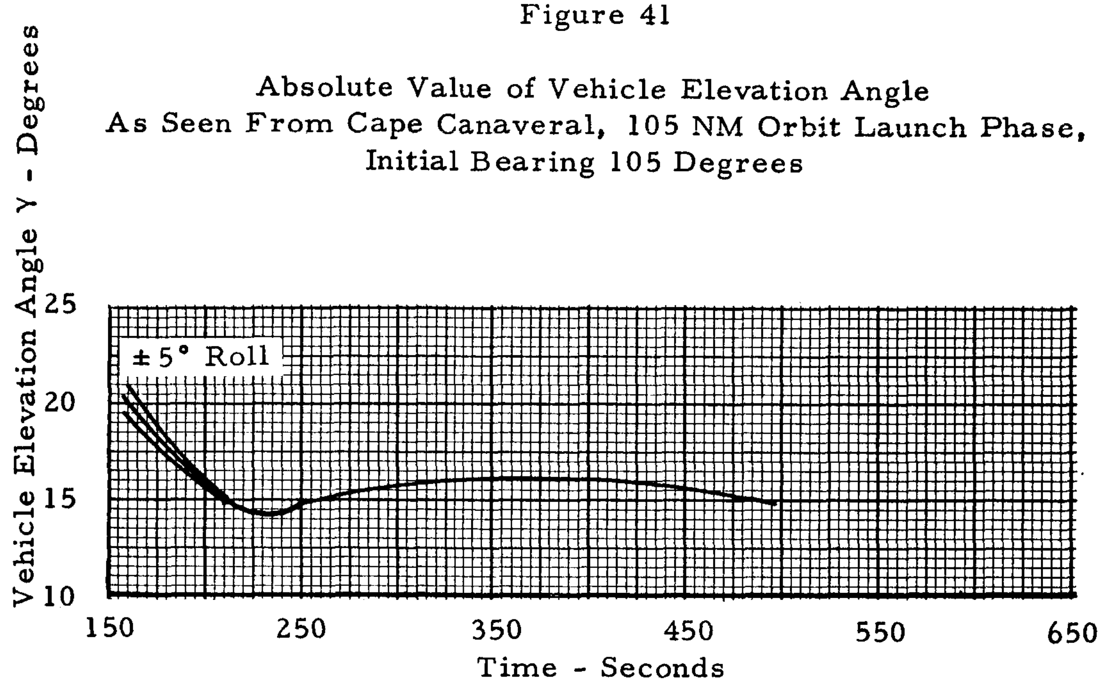

Figure 42

Absolute Value of Vehicle Elevation Angle
As Seen From Site Jupiter, 105 NM Orbit Launch Phase,
Initial Bearing 105 Degrees

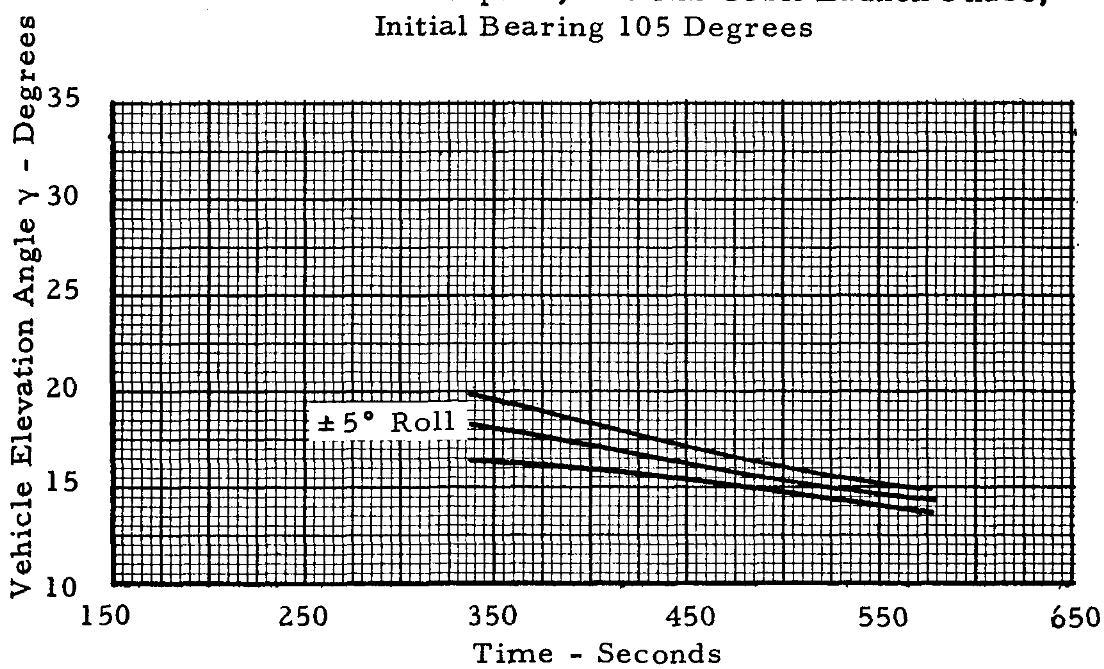

Figure 43 - Absolute Value of Vehicle Elevation Angle, γ As Seen From San Salvador, 105 NM Orbit Launch Phase, Initial Bearing 105 Degrees

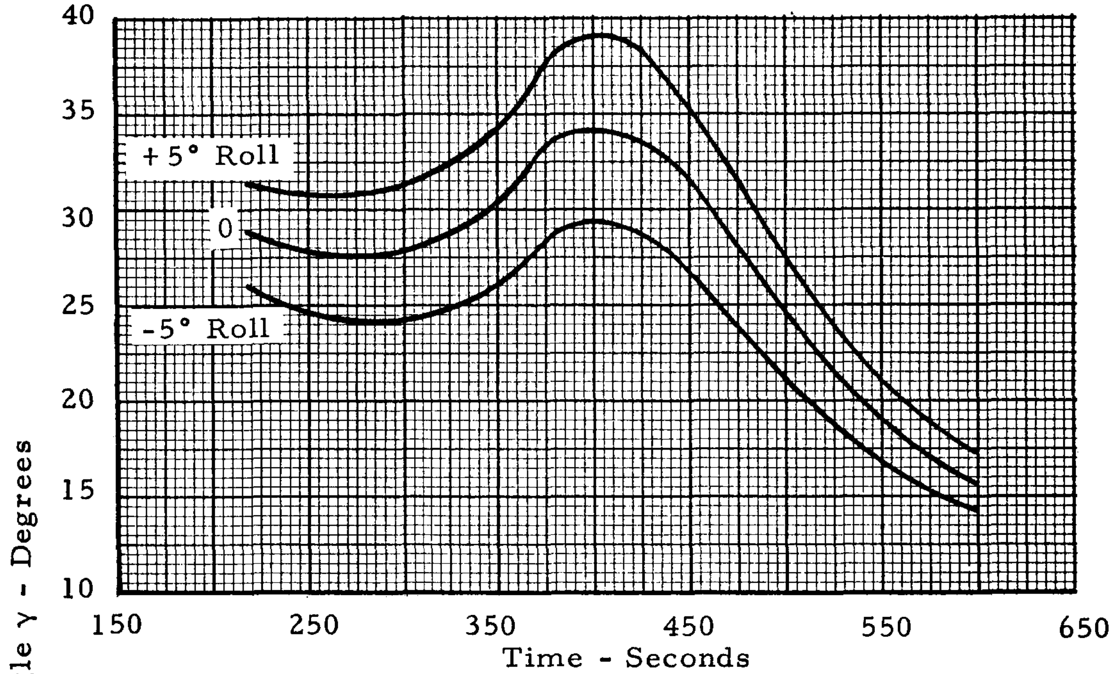

Vehicle Elevation Angle γ - Degrees

Figure 44 - Absolute Value of Vehicle Elevation Angle, γ As Seen From Grand Turk, 105 NM Orbit Launch Phase, Initial Bearing 105 Degrees

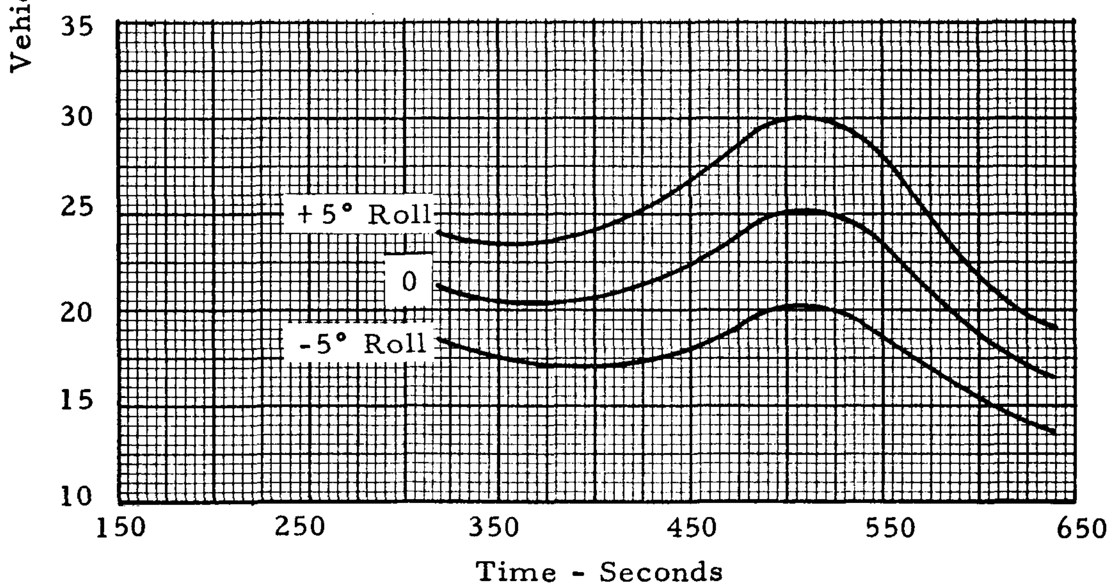

Figure 45 - Absolute Value of Vehicle Elevation Angle, γ As Seen From Bermuda, 105 NM Orbit Launch Phase, Initial Bearing 105 Degrees

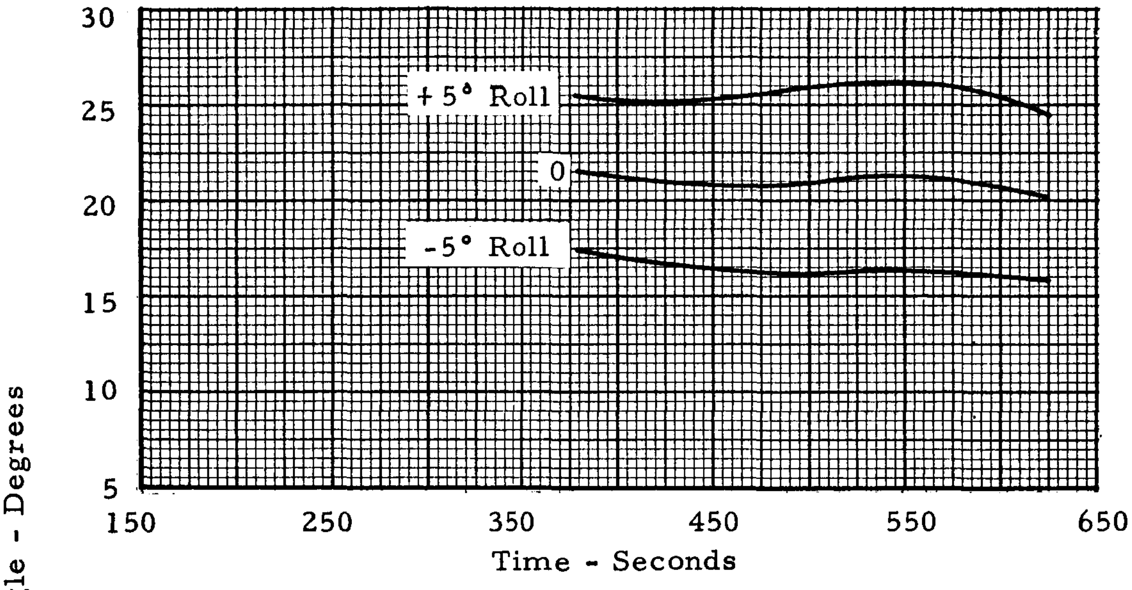

Figure 46 - Absolute Value of Vehicle Elevation Angle, γ As Seen From Antigua, 105 NM Orbit Launch Phase, Initial Bearing 105 Degrees

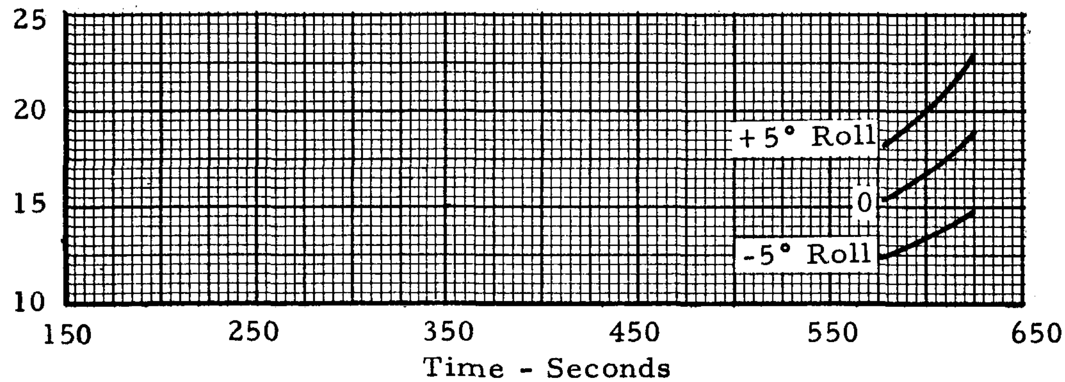

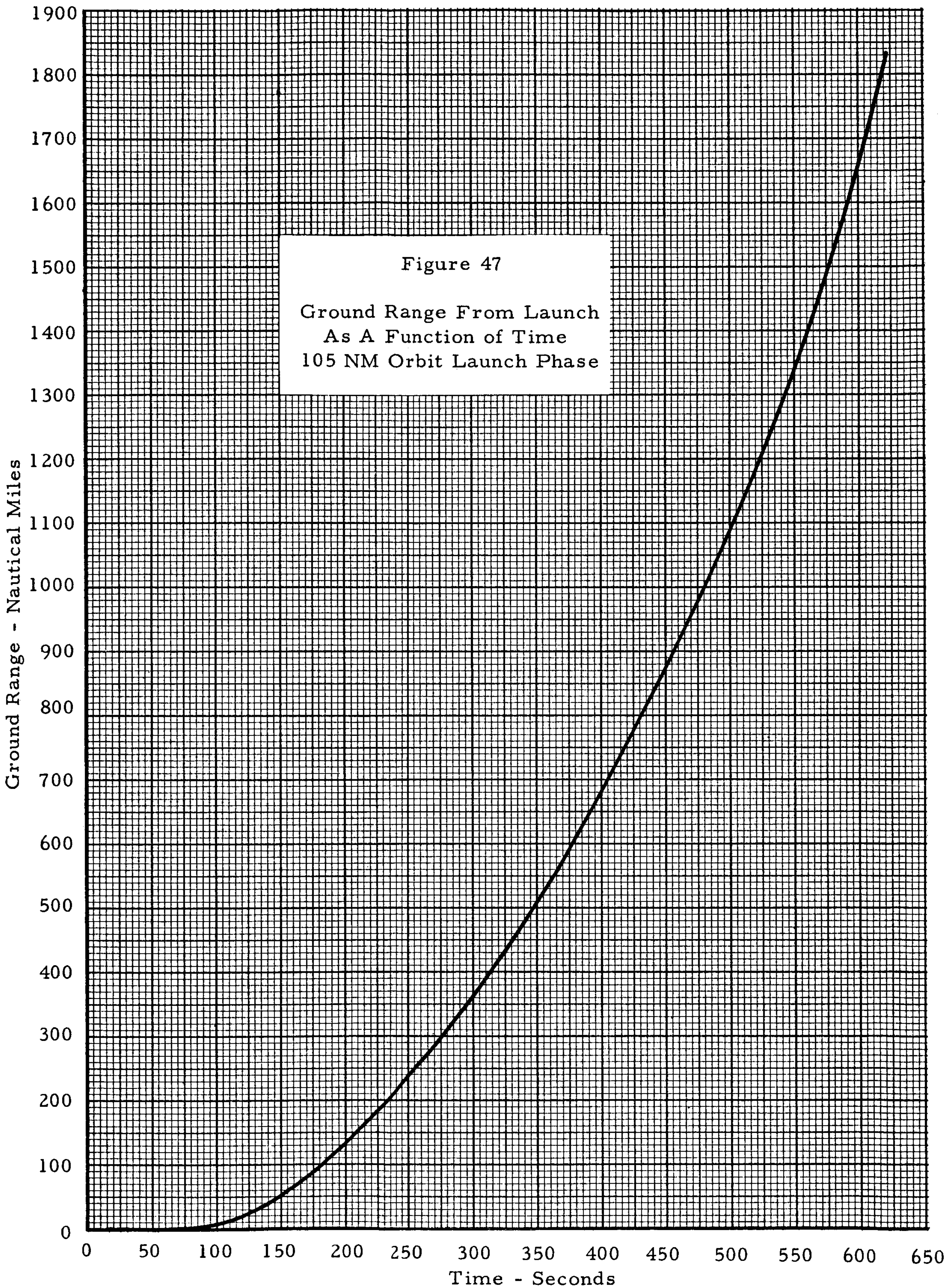

Figure 47

Ground Range From Launch
As A Function of Time
105 NM Orbit Launch Phase

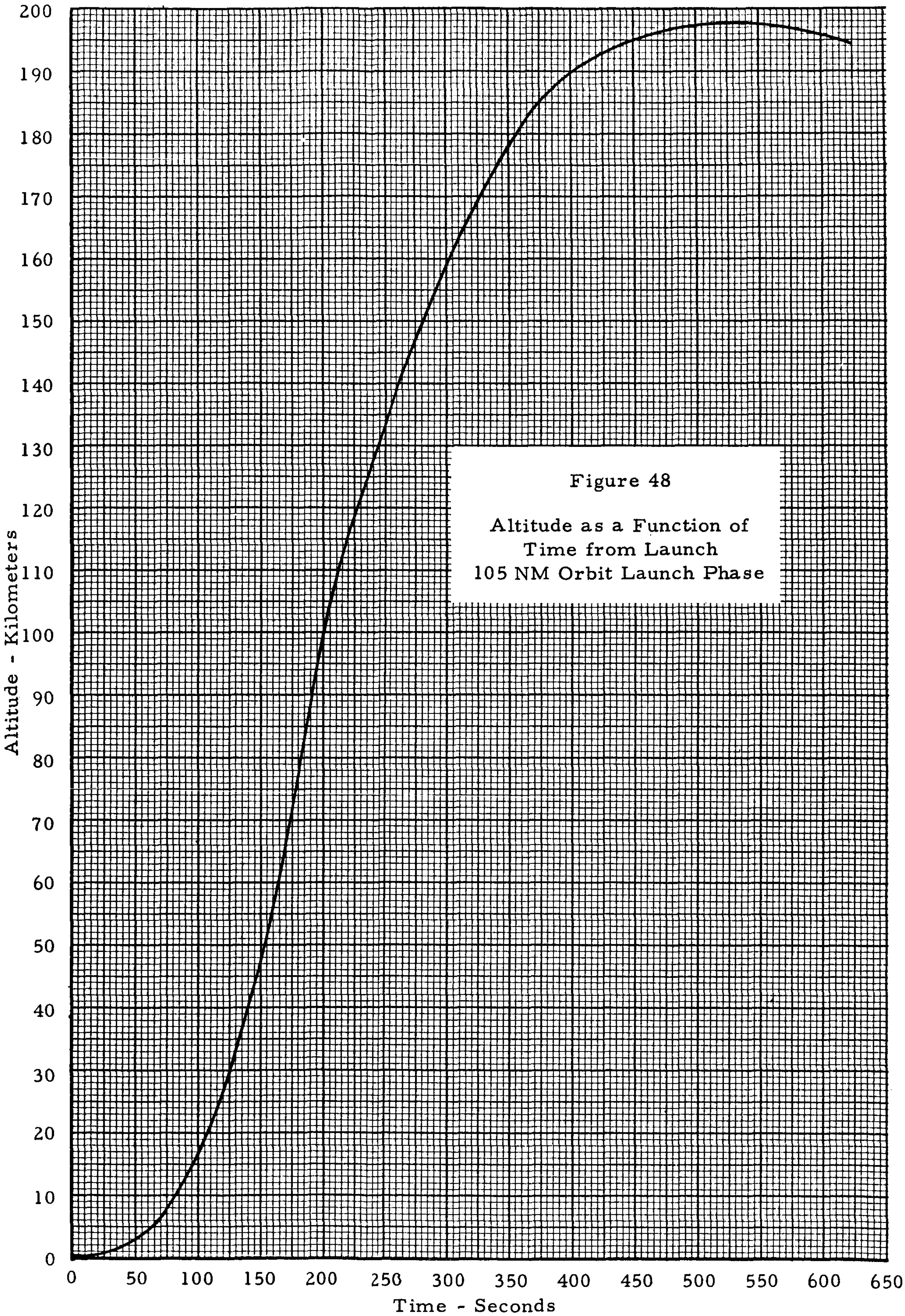

Figure 48

Altitude as a Function of
Time from Launch
105 NM Orbit Launch Phase

TABLE I

Maximum Values of Rate of Change of Range Rate, $\ddot{R}$, Azimuth Angle Rate, $\dot{\psi}$, Elevation Angle Rate, $\dot{\xi}$ and Aspect Angle Rate, $\dot{\eta}$

Station Name	Time* (secs)	$\ddot{R}$ (m/sec^2)	Time (secs)	$\dot{\psi}$ (deg/sec)	Time (secs)	$\dot{\xi}$ (deg/sec)	Time (secs)	$\dot{\eta}$ (deg/sec)
Cape Canaveral	475	16.0			170	0.30	160	0.17
Jupiter	200	20.8	205	0.83	177	0.32	180	0.80
San Salvador	465	39.3	435	0.83	330 515	0.20	425	1.25
Grand Turk	560	57.7	515	0.55	620	0.16	525	1.00
Bermuda	615	54.0	585	0.33	620	0.05		0.33
Antigua	623	50.0	624	0.52	618	0.12	625	1.00

*Approximate Time of Occurrence After Launch Time